

Volume estimation of soil stored in agricultural terrace systems: A geomorphometric approach

Sara Cucchiario^{a,b,*}, Guido Paliaga^c, Daniel J. Fallu^d, Ben R. Pears^e, Kevin Walsh^f, Pengzhi Zhao^g, Kristof Van Oost^g, Lisa Snape^h, Andreas Lang^h, Antony G. Brown^{d,e}, Paolo Tarolli^b

^a Department of Agricultural, Food, Environmental and Animal Sciences, University of Udine, Via delle Scienze, 206, 33100 Udine, Italy

^b Department of Land, Environment, Agriculture and Forestry, University of Padova, Agripolis, viale dell'Università 16, 35020 Legnaro, Italy

^c Research Institute for Geo-Hydrological Protection, National Research Council, Strada delle Cacce 73, 10135 Torino, Italy

^d Natural Sciences, Tromsø University Museum, Arctic University of Tromsø, Kvaløytveg 30, 7 Tromsø 9013, Norway

^e Department of Geography and Environmental Science, University of Southampton, SO17 1BJ Southampton, UK

^f Department of Archaeology, University of York, The King's Manor, Exhibition Square, York YO1 7EP, UK

^g Georges Lemaître Centre for Earth and Climate Research, Earth and Life Institute, UCLouvain, 1348 Louvain-la-Neuve, Belgium

^h Department of Geography and Geology, University of Salzburg, Salzburg 5020, Austria

ARTICLE INFO

Keywords:

Volume computation
Agricultural terrace systems
High-resolution topography
Geomorphological features

ABSTRACT

High-resolution topographic (HRT) techniques allow the mapping and characterization of geomorphological features with wide-ranging perspectives at multiple scales. We can exploit geomorphometric information in the study of the most extensive and common landforms that humans have ever produced: agricultural terraces. We can only develop an understanding of these historical landform through in-depth knowledge of their origin, evolution and current state in the landscape. These factors can ultimately assist in the future preservation of such landforms in a world increasingly affected by anthropogenic activities. From HRT surveys, it is possible to produce high-resolution Digital Terrain Models (DTMs) from which important geomorphometric parameters such as topographic curvature, to identify terrace edges can be extracted, even if abandoned or covered by uncontrolled vegetation. By using riser bases as well as terrace edges (riser tops) and through the computation of minimum curvature, it is possible to obtain environmentally useful information on these agricultural systems such as terrace soil thickness and volumes. The quantification of terrace volumes can provide new benchmarks for soil erosion models, new perspectives to stakeholders for terrace management in terms of natural hazard and offer a measure of the effect of these agricultural systems on soil organic carbon sequestration. This paper presents the realization and testing of an innovative and rapid methodological workflow to estimate the anthropogenic reworked and moved soil of terrace systems in different landscapes. We start with remote terrace mapping at large scale and then utilize more detailed HRT surveys to extract geomorphological features, from which the original theoretical slope-surface of terrace systems were derived. These last elements were compared with sub-surface information obtained from the excavations across the study sites that confirm the reliability of the methodology used. The results of this work have produced accurate DTMs of Difference (DoD) for three terrace sites in central Europe in Italy and Belgium. Differences between actual and theoretical terraces from DTM and excavation evidence have been used to estimate the soil volumes and masses used to remould slopes. The utilization of terrace and lynchets volumetric data, enriched by geomorphometric analysis through indices such as sediment conductivity provides a unique and efficient methodology for the greater understanding of these globally important landforms, in a period of increasing land pressure.

* Corresponding author.

E-mail address: sara.cucchiario@uniud.it (S. Cucchiario).

<https://doi.org/10.1016/j.catena.2021.105687>

Received 9 December 2020; Received in revised form 5 August 2021; Accepted 16 August 2021

Available online 6 September 2021

0341-8162/© 2021 The Authors. Published by Elsevier B.V. This is an open access article under the CC BY license (<http://creativecommons.org/licenses/by/4.0/>).

1. Introduction

Terraced landscapes can be viewed as both historical heritage and providers of ecosystem service, and as such they should be preserved across the globe if possible. They reduce slope gradient and increase the water infiltration in areas with moderate to low soil permeability, mitigate soil erosion, collect rainwater run-off, enhance nutrients and facilitate agriculture on steep slopes (Tarolli et al., 2014; Arnáez et al., 2015; Wei et al., 2016).

Terraced landforms fall generically under the term ‘agricultural terraces’ which include lynchets formed by the repeated action of ploughing/tillage and the gradual lateral transfer of cultivation sediments across low gradient slopes. The rationale for creating or using pre-existing natural terraces is a consequence of the need to cultivate steep slopes that are difficult to plough. These can take the form of deliberately constructed features with extensive sub-horizontal benches cut into hillsides and bounded by dry-stone walls (Brown et al., 2021). Terraces are commonly recognized as a crucial component of the agricultural landscape for their cultural value and their importance in food production in high-slope environments (Paliaga et al., 2016). Additionally, terraces represent the most obvious, widespread and profound anthropogenic alteration of the soil-slope system (effectively anthropogenic catenae) to the earth’s surface (Tarolli et al., 2019). Some recent research has focused on terraces as anthropogenic features where the original ground surface has been extensively remodelled (Rosenbaum et al., 2003), but in practice, it can be difficult to delineate areas of excavated ground and made ground. An open, but important question is how much they affect weathering and soil production rates since weathering is known to be related to factors including soil depth, soil density, structure, organic matter and age (Lin, 2011). Therefore, it follows that the estimation of soil volumes is important both practically and theoretically. The volume computation of these anthropogenically redistributed soils has a key role for several reasons: *i*) it is a measure of human landscape modifications, *ii*) construction of terraces involves alteration of the topography and redistribution of soil particles, creating colluvial soils enriched in nutrients and soil organic carbon (SOC; De Blécourt et al., 2014; Shi et al., 2019). Several studies have emphasized the potential of agricultural terraces to store C (Walter et al., 2003; Xu et al., 2015; Chen et al., 2020). For example, estimation from field sampling reported that terracing on average increased SOC stock by 25–55% (Walter et al., 2003; Welemariam et al., 2018; Zhao et al., 2021). Volume computation of soils stored in terraces is the starting point for the estimation of SOC stock. *iii*) terraces represent an available sediment source that must be estimated and considered in the planning of watershed management and risk mitigation. Indeed, slope changes have important implications for water infiltration, surface run-off and slope instabilities (e.g., soil erosion, shallow landslides, debris flow and flash floods) at local and catchment scales. Therefore, terrace construction and maintenance represent a potential reduction in the geo-hydrological hazards for agricultural landscapes on slopes and human infrastructure (e.g., population, buildings and roads etc.; Paliaga et al., 2020) and the methodology may be used together with others focusing on the state of conservation of stone walls (Cambi et al., 2021). However, a progressive decrease in maintenance (e.g., stone wall collapse; Preti et al., 2018a), construction in inappropriate areas, and increasing frequency of extreme weather events have made terrace systems one of the most erosion-prone agricultural landscapes with ‘dormant instabilities’ (Tarolli et al., 2014) that cause significant geo-hydrological risk. Understanding the volumes of material that extreme events could potentially mobilise can be used as benchmarks for numerical and physical modelling of erosion and soil formation process simulations in land degradation analysis of agricultural environments. Moreover, volume computations could also provide critical information in the design and construction of hard-line engineering works to reduce the risks posed by elemental exposure towards terraces.

Recent advances in remote sensing can contribute to the

development of more accurate methodologies that can assess terrace soil volumes by exploiting high-resolution topographic (HRT) technologies. These techniques have facilitated our ability to characterise and monitor terrace systems by identifying subtle sub-ocular geomorphological features. For example, Airborne Laser Scanning (ALS), which uses Light Detection and Ranging (LiDAR) technology, can map terrace systems over abandoned and vegetated areas and across large spatial scales (Sofia et al., 2014b; Godone et al., 2018), whilst Terrestrial Laser Scanning (TLS) permits a ground-based and detailed perspective of vertical terrace surfaces (e.g., dry-stone walls, steps etc.) along hillslopes (Camera et al., 2018; Cucchiaro et al., 2020a). In the last few years, the exploration of the Structure from Motion (SfM) photogrammetry technique paired with Multiview Stereo (MVS) algorithms (hereafter together referred to as SfM; Carrivick et al., 2016) in parallel with Uncrewed Aerial Vehicles (UAVs) have increased the possibilities for rapid, low-cost and very detailed surveys for terrace-complex monitoring at the landscape scale (Wei et al., 2017; Pijl et al., 2021; Tucci et al., 2019; Cucchiaro et al., 2020b). Moreover, the data fusion of HRT technologies (e.g., SfM and TLS data) allows us to overcome specific disadvantages of a single method under challenging contexts (e.g., steep slope and vegetated terrace systems; Cucchiaro et al., 2020a). From HRT surveys, it is possible to produce high-resolution Digital Terrain Models (DTMs) that supply quantitative land-surface metrics to analyse of terrace geomorphological features (Sofia, 2020) at different scales and detail. DTMs can be used to automatically detect terrace features using extraction algorithms (Diaz-Varela et al., 2014; Tarolli et al., 2014; Godone et al., 2018) based on specific geomorphometric parameters of terrace landscapes (e.g., surface derivatives such as maximum curvature that identified terrace edges). Furthermore, DTMs also help us to analyse instability phenomena in such steep-slope agricultural landscapes through effective geomorphometric index analysis of terrace systems in Geographic Information System (GIS) software. In this paper the authors and exploit all of these geomorphometric information approaches in the development of a fast-methodological workflow for the estimation of terrace volumes. The challenge and novelty of this work is the provision of a rapid and robust computation of terrace or lynchets soil volumes in different agricultural systems at the landscape scale. Moreover, this work analyses some possible applications of terrace soil volume computations, e.g., quantify the volume of sediments and associated SOC that could potentially be mobilized and exported downstream after a terrace failure. Such information is essential for policy makers and stakeholders responsible for maintaining agricultural terraces. The methodology starts from remote terrace system mapping at a large scale (using ALS) and then SfM-TLS data fusion was used to carry out more detailed surveys. The derived DTMs allow the extraction of useful geomorphological features from terrace slopes. In particular, moving the attention from edges to terrace riser bases through the computation of minimum curvature was hoped to identify an original theoretical surface of terrace systems, which is fundamental to the estimation of terrace soil volumes and understanding terrace histories.

2. Study areas: Terrace systems

In this study, the terrace computation approach has been tested on three agricultural terrace sites (Fig. 1): Martelberg in the Sint-Martens Voeren area of eastern Belgium (Fig. 1a, b and c), Soave-Fornace Michelin traditional vineyards (a Globally Important Agricultural Heritage Systems -GIAHS site) in the Veneto region of north-eastern Italy (Fig. 1d, and e) and San Fruttuoso Abbey terraces, along the slopes of Portofino promontory in the Portofino Regional Natural Park (Liguria region; Fig. 1f, g and h).

These sites are case studies for the TerrACE geoarchaeological research project (ERC-2017-ADG: 787790, 2019–2023; <https://www.terrace.no/>) that aims to create a methodological step-change in the understanding of agricultural terraces. This research project applies an integrated new scientific methodology to agricultural terraces across

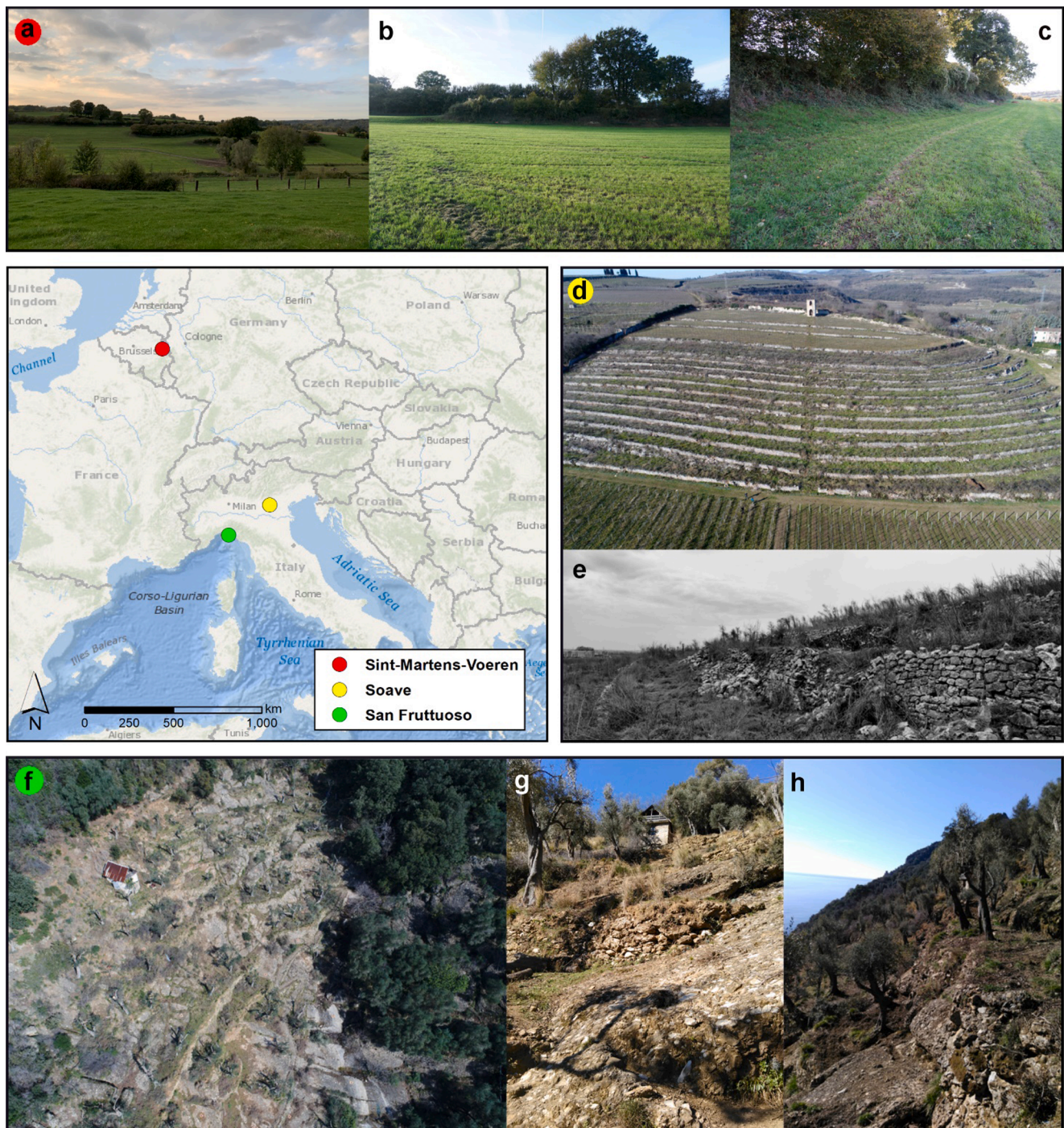


Fig. 1. Location of terrace study areas in Europe: (a) the vegetated braided lynchets of Martelberg in Sint-Martens Voeren, with (b-c) detail of the trees and shrubs that cover the terrace risers; (d) Soave-Fornace Michelin study area, characterised by dry-stone contour terraces with some collapses and shrubby vegetation (e); (f) San Fruttuoso Abbey terrace where stone walls are directly placed on bedrock (g-h) along the slopes of Portofino promontory in Liguria region.

Europe, bringing together landscape archaeology, geomorphology, and paleoecology. These terrace sites have been selected for analysis because they comprise different morphologies, landforms, features, slopes and present different problems in terms of potential instability and geo-hydrological risk.

2.1. Belgian lynchets/terraces

The Sint-Martens Voeren site covers 18 ha of hilly agropastoral land (an elevation range between 195 and 230 m) in eastern Belgium close to the Netherlands' border (see Fig. 1a, b and c). The agricultural landscape

across the valley is associated with three distinct surface gradient zones encompassing the hill-top (5–8%), dry valley bottom (8%), and a very steep mid-valley section (26%), and these areas exhibit very different sub-surface topographies and gradients resulting in distinctive agricultural landforms. On the shallower gradient hill-top and dry valley bottom areas, lynchets extend over large areas and are associated with lateral sediment transfer caused by ploughing, resulting in enhanced soil depth at field edges alongside hedged boundaries and occasional trees. In contrast, in the considerably steeper mid-valley area on the western side of the valley, two clear terrace structures occur, resulting in much smaller field sizes bounded by very large terrace risers covered with

trees, shrubs and dense herbaceous vegetation. Periodically ploughed sloping pastoral land surrounds these features. Across the wider landscape, the extent of low-gradient land suitable for cultivation across the hill-tops and valley bottoms could have been utilized without the necessity to include the significantly more awkward, steeper mid-valley areas. A rationale for their inclusion, other than the need to occupy the maximum available land, was probably due to their pre-existence in the landscape. The terrace sub-surface is characterized by weathered chalk, occasionally capped by flinty colluvium redeposited from the surrounding hill-tops. The Mesozoic (Cretaceous) chalk crops out in a series of sub-horizontal benches that have been modified into terraces and lynchets (Nyssen et al., 2014). The nature of the basal chalk geology, much like other limestone landscapes, includes a relatively optimum horizontal to sub-horizontal bedding resulting in ladder-like steps with superimposed superficial sedimentation. At this site, this probably occurred during the Pleistocene and early Holocene and helped to create the features used in agriculture in later years. Indeed, a distinct benefit of these terraced areas over the surrounding landscape would likely have been the soil's relative stability. Detailed sub-sampling in the field enabled a specific characterisation of sub-surface topography and agricultural landforms across the site (further details in the following sessions).

2.2. Soave- Fornace Michelon dry-stone terraces

Research at Fornace Michelon in the Soave municipality in north-eastern Italy was conducted across a 3.5 ha area with an elevation range between 80 and 115 m and an average slope of 35% (see Fig. 1d and e). Historically, the numerous frequently abandoned and collapsing dry-stone contour terraces with shrub vegetation (Fig. 1d) across the steep slopes have been used to develop vineyards. The general geology of the Soave region consists of Cretaceous Limestones capped by Paleogene Basalts. The faulting and subsequent erosion of these layers produce the mosaic of calcareous and volcanic soils upon which the Soave vineyards are founded. The Fornace Michelon locality, sampled for this study, is located on a low outcrop of tabular chert-rich limestone. The soil has eroded entirely across several areas, exposing the bedrock. The terraces at Fornace Michelon appear to be relatively recent, being absent from the Napoleonic cadastral survey. The terraces are arranged around a central path or ramp leading to a square-built tower of relatively recent construction. The main gate through the perimeter wall of the terraces communicates with the gate of an early 19th-Century villa across the modern road, suggesting the construction of the terrace dates to this period.

2.3. San Fruttuoso Abbey site terraces

The San Fruttuoso Abbey terraces in north-western Italy are located along the southern slopes of the Portofino promontory. The research took place across a 0.25 ha area ranging in elevation between 92 and 148 m with an average slope of 88% (see Fig. 1f, g and h). The site provides excellent examples of ancient human modification of high gradient slopes along the coast. In this zone, due to the high steepness of the slopes, the dry-stone terraces were directly placed on the bedrock forming pocket type or small braided terraces (Paliaga et al., 2020). The bedrock is Portofino Conglomerates (Faccini et al., 2018) which contains pebbles that are primarily calcareous/limestone and secondarily sandstone, ophiolites, gneiss and cherts, while the matrix is calcareous sandstone with quartz and clay elements. Two NW-SE and NE-SW oriented faults systems affect the bedrock, causing fractures that can dislocate rocky blocks exceeding 10 m (Paliaga et al., 2016). Furthermore, the geology creates conditions for a remarkable subterranean water circulation with small springs occurring across the terraces. The presence of terraces in this area has been linked to the medieval historic buildings and religious structures, in particular, the San Fruttuoso Abbey which was constructed at the beginning of the 10th Century by the Greek

monks. Later documents describe the land use and agricultural practices from the mid-13th Century that were developed by the Order of Saint Benedict. To make cultivation possible, the original steep slope profile was modified with dry-stone terraces that required constant maintenance activity, which was performed until the middle of the 20th Century (Paliaga et al., 2016). The progressive abandonment of agricultural practices has caused a high threat of erosion and gravity-induced processes (rockslides) which accompany terrace collapse.

3. Methods

3.1. High-resolution topographic data for terrace location

The availability of large-scale topographic ALS datasets allowed the construction of high-resolution DTMs and a shaded relief map that were used for an initial and rapid assessment of the location of terraces. For the Belgian site and Soave-Fornace Michelon study area, DTMs at 1 m resolution were provided by Flanders Information Agency (ALS survey year: 2014) and Environmental Italian Minister (ALS survey year: 2009) respectively, while for San Fruttuoso Abbey a DTM at 0.5 m resolution was used, extracted by the survey performed under the H2020 project RECONNECT (ALS survey in February 2020).

Once terraced positions were identified, a higher resolution surveys using SfM and TLS techniques were carried out to better identify and locate terrace components (e.g., surface, riser edge, and base) at a more detailed scale, exploiting geomorphometric information and orthomosaics (see next Section 3.2). At the Belgian and Soave-Fornace Michelon sites, integrated TLS and SfM were conducted to overcome particular detection problems associated with the complex topography and land-cover conditions (see Cucchiaro et al., 2020a). TLS allowed terrace wall and lynchets riser detection, while the flat terrace zones (treads) and the broader landscape was surveyed from UAV-SfM. In contrast, the extreme nature of the topography at San Fruttuoso Abbey, including the steep slope and inaccessibility of some areas, meant that only the UAV-SfM survey data could be reliably used.

3.1.1. Data acquisition

Before data acquisition, SfM and TLS targets or Ground Control Points (GCPs) were distributed throughout the study areas (Fig. 2a, b and c) in flat zones but also on vertical surfaces so that GCPs were visible from different points of view (i.e., nadir and oblique images and TLS positions). The GCPs position, which is fundamental for georeferencing and co-registration process, and error assessment, were surveyed using a Reach RS (Emlid Ltd.; real-time kinematic-RTK solution) with the EUREF-IP network in NRTK mode (network of permanent Global Navigation Satellite System-GNSS stations) for the Belgium study area. For the Italian areas, a GeoMax Zenith 40 GNSS allowed us to survey all targets.

The TLS surveys were carried out at sites in Belgium and Soave-Fornace Michelon with a Leica P50 TLS (Fig. 2d). We completed the Belgian SfM survey using a custom-built Quadcopter equipped with a DJI A3 flight controller and a Sony ILCE-6000 camera (24 Mpixels, focal length 16 mm, sensor size APS-C 23.5 mm × 15.6 mm). GCPs could only be distributed along the western side of the study area due to the inaccessibility of the eastern side; therefore, the direct georeferencing technique was used to reconstruct the morphology of specific parts of the study area (more details in Cucchiaro et al., 2020a). For the Italian SfM surveys, nadir and oblique UAV images were collected with a DJI Zenmuse X4S camera (20 Mpixels, focal length 8.8 mm, 1-inch CMOS Sensor) mounted on a professional quadcopter (DJI Matrice210v2; Fig. 2e). GNSS, SfM and TLS arrangements are summarised in Table 1.

3.1.2. DTM generation and error analysis

TLS data were processed using Leica Cyclone 9.4 software, where the multiple scans were manually filtered, georeferenced and co-registered using targets and the iterative closest point (ICP) automatic algorithm.

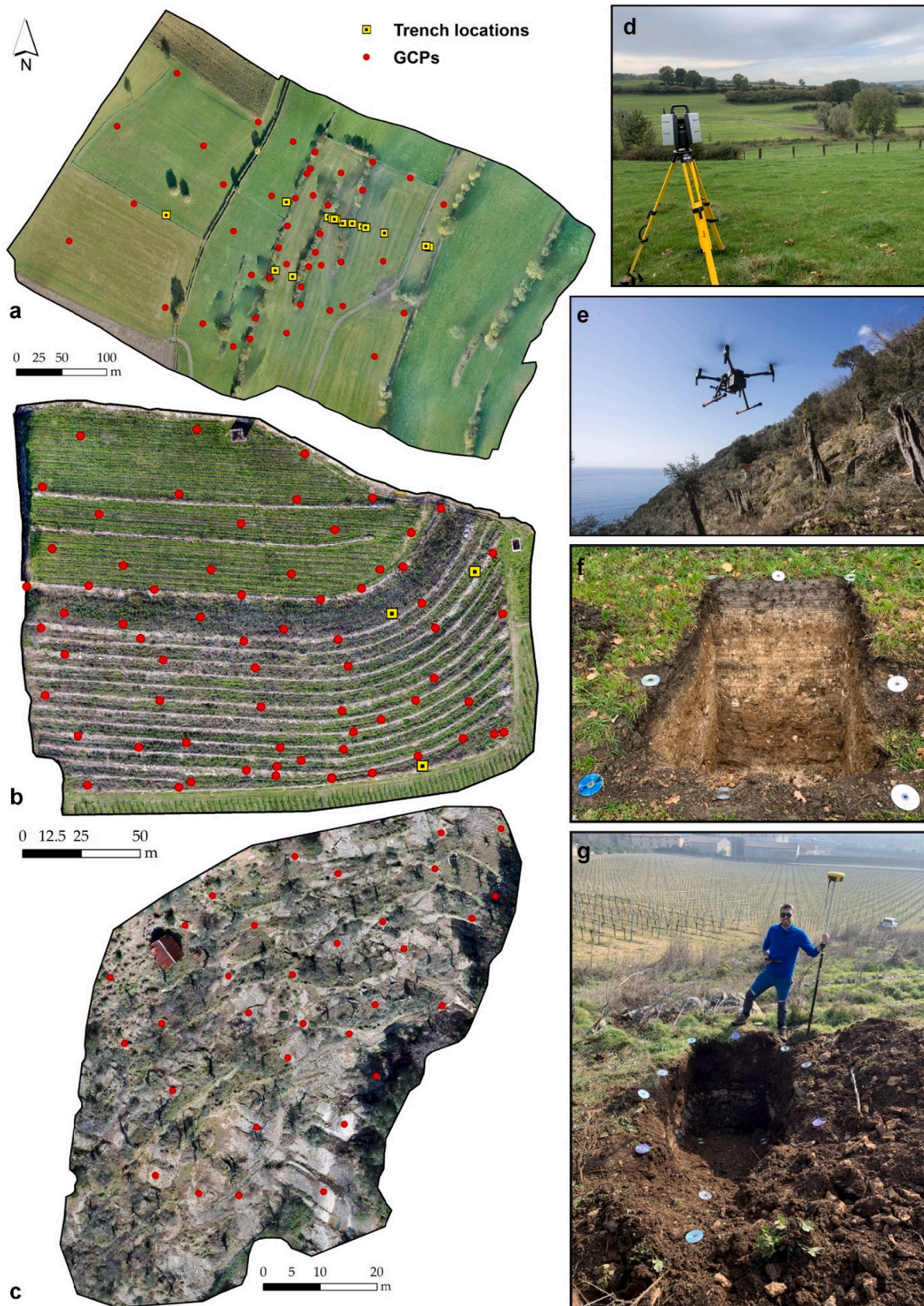


Fig. 2. Detailed terrace scale mapping of study areas using SfM and TLS technique. Orthomosaics, GCPs and trench positions of the Belgian (a), Soave-Fornace Michelin (b), and San Fruttuoso Abbey (c) study areas; (d) The Leica P50 used for TLS surveys, during a scan of the Belgian vegetated braided lynchets; (e) The quadcopter DJI Matrice210v2 used in Italian SfM surveys; (f-g) Examples of the trenches dug in Belgian and Soave-Fornace Michelin study areas, during detail SfM surveys.

Table 1
Main characteristics of SfM and TLS surveys.

Study Area	Belgium	Soave-Fornace Michelon	San Fruttuoso Abbey	
GNSS survey	Date	October 2019	December 2019	February 2020
	Area (ha)	18	3.5	0.25
	Number of targets	60	67	32
	Positional Accuracy (X, Y – Z) (m)	<0.05	0.03–0.04	0.03–0.04
	Reference system	WGS84/UTM zone 31N (EPSG: 32631)	RDN2008/UTM zone 32N (EPSG: 7791)	RDN2008/UTM zone 32N (EPSG: 7791)
SfM survey	Number of images	1219	632	546
	Flight Height (m)	20–45	25–35	35
	Ground Simple Distance (GSD) (m)	0.005–0.015	0.006–0.008	0.008
TLS survey	Accuracy (m)	1.6 mm@10	1.6 mm@10	–
	Maximum Range Mode (m)	120	270–570	–
	Scan Rate (Points/s)	1,000,000	250,000–500,000	–
	Number of Scans	7	6	–

The SfM datasets were processed to extract the 3D point clouds and orthomosaics from the images through Agisoft Metashape Pro v 1.6.2 (Fig. 2a, b and c). The georeferenced point-clouds were imported into the CloudCompare software (Omnia Version 2.10.2; <http://www.danIELGM.net>) to be filtered for outliers, vegetation, and unwanted objects. For the Belgian and Soave-Fornace Michelon sites, the TLS and SfM point clouds were co-registered to minimise residual inaccuracies of the georeferencing process and finally merged, generating data-fusion point clouds (more details in Cucchiaro et al., 2020a). The point clouds were decimated through the geostatistical Topography Point Cloud Analysis Toolkit (ToPCAT), successfully used in several studies (e.g., Javernick et al., 2014; Vericat et al., 2014), to reduce the point cloud into a set of non-overlapping grid-cells, calculating the statistics for the observations in each grid. The minimum elevation within each grid cell was taken to be the ground elevation, and a grid cell of 0.10 m was selected to regularise the data set as in Brasington et al., (2012). The decimated point clouds were used to calculate a Triangular Irregular Network (TIN) converted to raster through a natural neighbour interpolator, resulting in one DTM for each study area.

Determining error in assessment data was fundamental for highlighting possible bias, and calculating the accuracy and precision of outputs. A bootstrapping resampling (1000 times) approach (Marteau et al., 2017) was chosen to analyse output accuracy and precision. One-third of the GCPs were randomly selected as CPs (Control Points) to estimate the quality of the SfM point clouds and provide an independent measure of uncertainty for each point (i.e., the residuals or the difference between the real coordinates of this point and the modelled values; Cucchiaro et al., 2018). To assess uncertainties usually caused by filtering from the classification of into-ground and off-terrain points as well as in the gridding process, especially in the vertical component, a statistical comparison was calculated between Z values of CPs (randomly selected) and the equivalent Z value measurements extracted from DTMs. This approach permits a robust assessment of the accuracy of measures that are not influenced by outliers, including the Normalized Median Absolute Deviation (NMAD).

3.2. Mapping of terraces and identification of their sub-surface origins

DTMs provide useful geomorphometric parameters that reveal the topographic characteristic of terrace landscapes, being characterised by a much sharper and linear shape than natural terrain features (Sofia et al., 2014b). Terrace systems represent outliers within the derived geomorphometric parameters (e.g., surface derivatives such as curvature); therefore, this information can be used to automatically extract particular features from DTMs through a statistical threshold of the

surface derivatives probability density functions. The method of terrace extraction from raw data (Tarolli et al., 2014; Sofia et al., 2014a) involves the use of the boxplot approach (Tukey, 1977), and the identification of outliers as points that verify Equation (1):

$$C_{max} > Q_{3C_{max}} + 1.5 \cdot IQR_{C_{max}} \quad (1)$$

where C_{max} (Wood, 1996) is maximum curvature calculated by solving and differentiating a quadratic approximation of the surface as proposed by Evans (1980), $Q_{3C_{max}}$ and $IQR_{C_{max}}$ are the third quartile and the interquartile range of C_{max} , respectively. The maximum curvature was chosen because terraces can be considered as ridges on hillslopes, and this geomorphometric parameter can easily identify the terrace riser edge from ALS-DTM at large scale. A moving window size (k) was considered for the calculation of curvature to reduce the effect of noise and small-scale variation in the DTMs. The window sizes (19 m for Belgium; 5 m for Soave-Fornace Michelon, and 9.5 m for San Fruttuoso Abbey) were chosen in relation to the maximum size of the terrace or lynchet features present at each site (6 m for Belgium; 1.5 m for Soave-Fornace Michelon and 3 m San Fruttuoso Abbey). Such an approach follows the indication of Tarolli et al., 2012, who demonstrated that an optimal window size for curvature should be about twice three times the maximum size of the investigated features.

The higher resolution DTMs and orthomosaics, realized from SfM-TLS surveys, provided key information for the detailed study of terrace morphology, particularly across riser edges and riser base locations. SfM-TLS DTMs were used to automatically extract stone wall or lynchet riser bases as high negative curvature zones following Equation (2):

$$C_{min} < Q_{3C_{min}} - 1.5 \cdot IQR_{C_{min}} \quad (2)$$

where C_{min} is the minimum curvature that underlines concave elements. Window sizes across the three sites (18.1 m for Belgium, 4.5 m for Soave-Fornace Michelon and 9.1 m for San Fruttuoso Abbey) were between 2 and 3 times the size of the investigated features, as suggested and optimally tested in previous work (e.g., Tarolli et al. 2012). After the identification of the terrace riser bases, using minimum curvature of DTMs, the extracted features were verified through the detailed orthomosaics at 0.02 m resolution obtained from SfM surveys. Then, the extracted terrace riser bases were converted into 3D contour lines and used to reconstruct a possible original surface (e.g., bedrock; Fig. 3) through their interpolation along a slope. This allowed the construction of theoretical surfaces (TS; Fig. 3) that could be used to calculate terrace volumes.

To verify the accuracy of the extracted features, the values of the

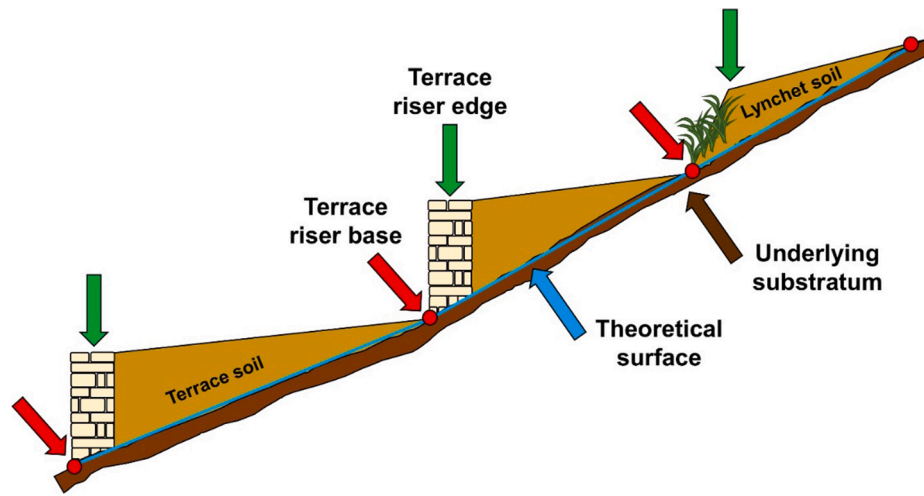


Fig. 3. Schematic drawing of a terrace or lynchet slope profile used as framework to terrace volume computations.

terrace riser edge and bases estimated through curvature were statistically analysed, testing the correlation between features classification and what was observed in the field. Two different analyses were performed: the quality index (Heipke et al., 1997) and Cohen's kappa standard accuracy ($k(X)$; Cohen, 1960). Both tests aimed to verify if a pixel classified as terrace riser edge or bases by the curvature method falls in areas obtained by digitizing shapefile manually drawn polygons based on the orthomosaics where terrace riser edge or bases were present.

3.3. Data validation using excavation and core information

To validate in broad terms the modelled TS and volume computations at each site, we excavated test pits and coring along cross-sections (Fig. 2f and g) which allowed a rough determination of absolute depths to bedrock geology or a superficial substratum in a quickly and raw way respect to geophysical measurements. As well as elucidating the chronology, construction, form, and function of the terraces (Brown et al., 2021), these sample points also enabled a comparison of sub-surface information measured by the GNSS survey and variations in the depth of TS to calculate errors in terrace volume calculations.

3.4. DTM of differences and volume computations

The difference between the actual terrace surface, using SfM-TLS, and the theoretical survey of sub-surface topography enabled the calculation of terrace volume. Furthermore, the modelled DTM of difference (DoD) could also be used to estimate the presence and extent of remodelled terrace soil overlying the basal geology. This calculation assumes that the riser bases sit on or near the bedrock head and that the bedrock head has a planar surface between these points. If in a small number of cases there is a gap of lower B-C horizon soil under the terrace bases, this makes the volume estimates a bit on the low side, therefore the soil estimations can be considered as minimums. DTM uncertainty and error propagation were considered in the analysis to obtain reliable DoDs and to discriminate between the actual difference in surface elevation and background noise. The significance of DoD difference was thresholded by applying a minimum level of detection ($minLoD$). Changes above $minLoD$ were considered real, but when the changes were below the $minLoD$ these were considered uncertain and not used in the final computation (Brasington et al., 2003; Lane et al., 2003). These DoDs were called the thresholded DoDs and were generated using the GCD software for ArcGIS (Wheaton et al., 2010). The uncertainty level of each DTM and the related theoretical interpolated surface was identified incorporating the corresponding SfM-TLS DTM errors, in particular, the

highest error value in the calculated metrics (i.e., Root-Mean-Square Error; RMSE) to ensure a more precautionary approach. The following Equation (3) computed the associated error on the DoD estimates (Vericat et al., 2017):

$$minLoD = t\sqrt{(\varepsilon_{DTM})^2 + (\varepsilon_{TS})^2} \quad (3)$$

where ε_{DTM} and ε_{TS} are the errors estimated for the SfM-TLS DTMs and the related theoretical interpolated surfaces, respectively, and t is the t -score (for a conservative approach a value of $t = 1.96$ was used, corresponding to a confidential interval of 0.95). Thresholded DoDs provide a difference in elevation for each grid cell; thus, knowing the size of each cell, the elevation changes were converted to volumes. Volume data was converted into terrace soil mass using bulk density information of the original material collated from the sample trenches excavated at Belgium and Soave-Fornace Michelon (Fig. 2f and g). In contrast, for San Fruttuoso Abbey, the value was derived from an existing source (Rellini et al., 2017).

3.5. Sediment connectivity analysis

The volume estimations derived from DoDs can be very useful for terrace management and assessments of geo-hydrological hazards, for example exploiting geomorphometric index as the Index of Connectivity (IC) proposed in Borselli et al., (2008) and Cavalli et al., (2013). IC is intended to represent the potential sediment connectivity between hillslopes and features, which act as targets or sources for transported sediment, and different parts of the catchment. IC is defined as (Eq. (4)):

$$IC = \log_{10} \left(\frac{D_{up}}{D_{dn}} \right) \quad (4)$$

where D_{up} and D_{dn} are the upslope and downslope components of connectivity, respectively. D_{up} is the potential for downward routing of the sediment that is produced upstream. This is dependent on the upslope contributing area, mean slope and terrain roughness. D_{dn} considers the flow path length that a particle has to travel to arrive at the nearest target (e.g., terrace) and it depends on path length, terrain roughness and gradient along the downslope path. This index can be used to identify the upstream area potentially connected in terms of sediment source within particular zones of terrace systems, for example, areas of dry-stone wall collapse. Indeed, knowing the connected area and computing specific DoDs for this part, it is also possible to quantify the volume of sediments and associated SOC that could potentially be mobilised and exported downstream after a terrace failure in time. This

represents a possible and suitable application of terrace soil volume estimates.

4. Result and discussion

4.1. Terrace mapping

The level of detail generated by the combination of high-quality SfM and TLS surveys enabled the modelling of accurate DTMs (Fig. 5), adequate for identifying topographic features without a loss of data from these complex topographic systems. Indeed, TLS data also provided a more accurate representation of sub-vertical surfaces covered by vegetation, especially across the sharp riser areas of terraces. At the same time, the UAV-SfM survey demonstrated subtle topographic variation over a wider area and particularly across flatter areas (Cucchiaro et al., 2020a). Table 2 summarises the point quality analysis of the GCPs and CPs in terms of precision, accuracy, and georeferencing error for each of the SfM and TLS processes carried out. The ICP errors obtained in CloudCompare software for the SfM-TLS co-registration processes show RMS values of 0.045 and 0.068 m for the Italian and Belgian sites, respectively. Moreover, Table 2, shows the DTM errors for each study area, underlining the high quality of the final outputs obtained from SfM and TLS surveys through the comparison with CPs measured in the field.

The availability of large-scale topographic ALS datasets allowed the rapid identification of terrace edges at each site (Fig. 4). These are perfectly visible along the slopes, and the statistical analysis through the quality index and Cohen's kappa standard accuracy (Table 3) confirmed the validity of the methodology. Indeed, the statistical results indicate an overall consistency between the extracted values of maximum curvature and the referenced features for all three study areas. Table 3 shows high values of $k(X)$ and a quality index that highlighted substantial agreement. Slightly lower statistical values were recorded for the study area in Belgium, where heavily vegetated lynchets/terraces were present, and the identification of their riser edge parts using orthomosaic was not easy. The methodology also worked in the San Fruttuoso Abbey study area, where terraces do not possess regular, uniform features. On the other hand, the best statistical results (Table 3) are found for the study area in Soave where the terraces have very regular shapes and were easily identifiable even from orthomosaic. Vital elements for automatic detection of terrace features are: data accuracy and resolution, which must be suitable for distinguishing terraces from noise. For example, vegetation cover in abandoned terrace systems creates background noise for the curvature extraction process (as in some parts of Soave-Fornace Michelon system; Fig. 4b), noise which does not belong to the linear shapes of terraces, but may have been generated by sub-optimal filtering of ALS data.

Table 2

Errors assessed for SfM and TLS point clouds, and their derived DTMs. For SfM surveys, the bootstrapping technique applied in Agisoft Metashape after all of the iterations provides the mean of the residuals (mean absolute error; MAE) as an indication of the accuracy of the georeferencing process and the point cloud when the GCP and CP residuals are used, respectively, while the standard deviation of the residuals (SDE) yields an indication of the precision. For the TLS surveys, georeferencing process's final error in the Cyclone software is reported in terms of RMS.

	TLS point cloud Georeferencing GCPs RMS	SfM point clouds						DTMs					
		Accuracy CPs			Precision CPs			Georeferencing GCPs					
		MAE (m)			SDE (m)			RMSE _{3D} ¹ (m)		MAE (m)		SDE (m)	
		X	Y	Z	X	Y	Z	MAE	SDE	RMSE ² (m)	NMAD ³ (m)		
Belgium	0.068	0.014	0.015	0.052	0.070	0.013	0.011	0.025	0.068	0.063	0.073	0.075	0.069
Soave-Fornace Michelon	0.045	0.013	0.014	0.019	0.034	0.010	0.011	0.014	0.031	0.024	0.026	0.040	0.035
San Fruttuoso Abbey	–	0.017	0.017	0.025	0.043	0.014	0.011	0.018	0.038	0.045	0.039	0.049	0.035

¹ RMSE_{3D} (3D Root-Mean-Square Error; Remondino et al., 2017) of GCPs and CPs computed along the x, y, and z directions.

² The outliers were removed by applying a threshold (2 times the RMSE) selected from an initial calculation of the RMSE measures (Höhle and Höhle, 2009).

³ NMAD: proportional to the median of the absolute differences between errors and the median error (Höhle and Höhle, 2009).

The use of more detailed and slope scale surveys (i.e., SfM-TLS) significantly improved the analysis of terrace morphology signals because they provided higher quality DTMs with more accurate control of errors and noise filtering and higher resolution orthomosaics that allowed a finer check of the feature extraction process. The negative curvature values extracted from higher resolution SfM-TLS DTMs effectively identified the terrace riser base as it is possible to see in Fig. 5. Moreover, the extraction process's statistical assessment shows the high values of $k(X)$ and quality index in Table 3 for all study areas, underlining a further degree of agreement between the terrace riser base in the field and the features extracted by curvature method using more detailed surveys. The 3D contour lines extracted from curvature data closely follow the terrace riser base profile in each different study area (Fig. 5a, b and c), and the SfM orthomosaics confirmed their correct position (Fig. 5d, e and f).

4.2. Original terrace surfaces and field validation

Determining the accuracy of the results of terrace base detection using extant surface geomorphological features (as was done in Table 3) was fundamental for the reconstruction of a legitimate sub-surface topography. At each of the study sites, profile comparisons between real DTMs and TS modelling of the terrace bases demonstrate distinctive results relating to original terrain profiles (Fig. 6). The interpolation surfaces faithfully followed the terrain profiles (extracted in Fig. 5) from the terrace riser bases, allowing the identification of the possible substrate and the initial slope along which the terraces and lynchets were built. The profile of the TS is almost always under the terrace layer, except for isolated incidences where the two surfaces are close together in low-slope areas (e.g., C1, C2 and C8 in Belgium; Fig. 6a) and across areas of denser vegetation, masking terrace identification (e.g., T2 at Soave-Fornace Michelon; Fig. 5b).

Across each sample site area, the excavation of test pits and extraction of sediment cores (Fig. 5; Table 4) added sub-surface information that supported in broad terms the hypothetical depth values calculated by the TS. This compatibility was undeniable at the Belgian site where seven 1 m² test pits and eight hand-augered sediment cores revealed the nature of the sub-surface topography in detail (Fig. 7; Table 4) and demonstrated an excellent correlation with the TS surface model. Across the hilltop, two test pits (T1 and T2) revealed moderately thick agricultural deposits (c. 0.45–0.55 m) in low lying lynchets landforms, which lay directly on stony clay and coarse gravel geology. The TS depth values for T1 trench corresponded well to this (since T1 data was used as the bedrock starting point of the TS upslope; see Table 4), while in T2 there was an overestimation of the existing terraced volumes. Beneath the Cenozoic clay and gravel geology, the Mesozoic chalk bedrock (Pirson

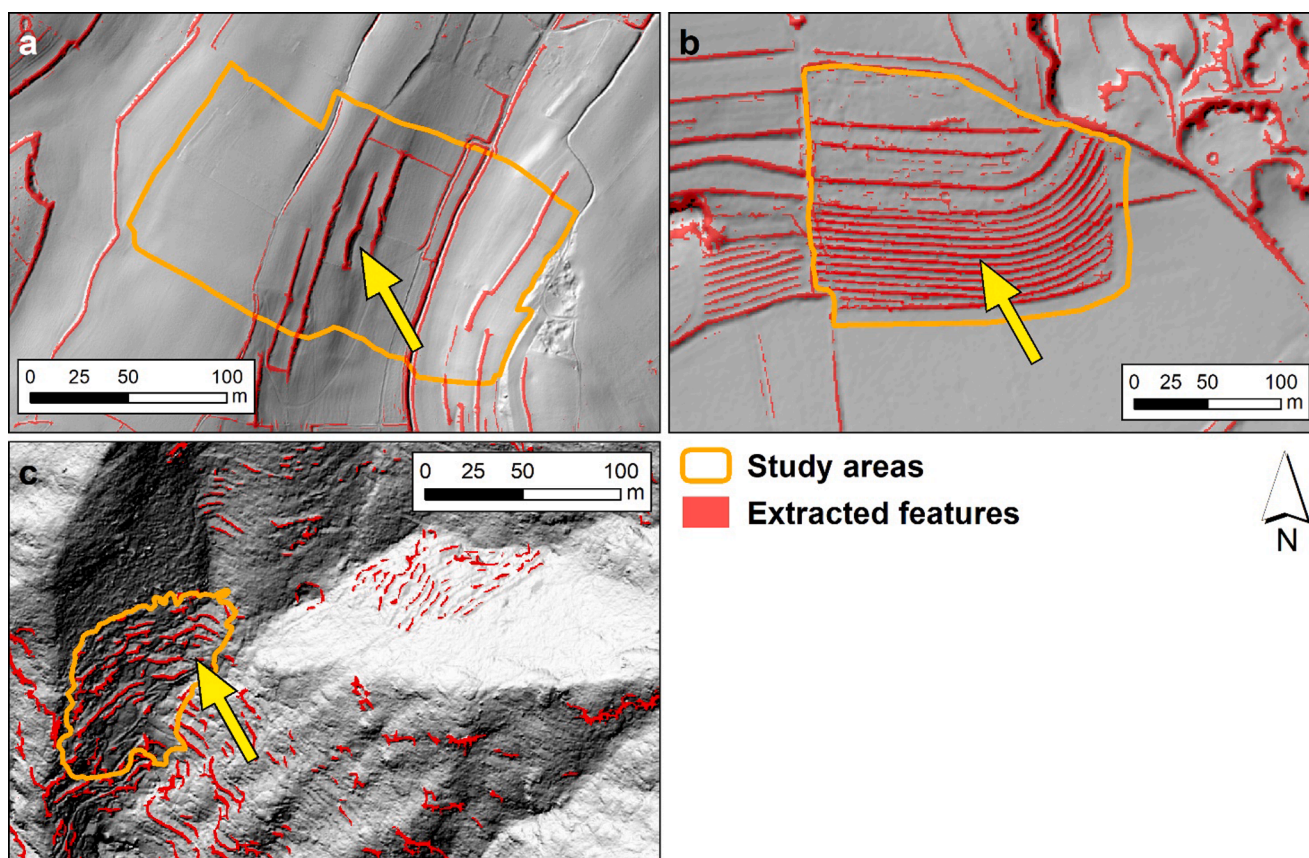


Fig. 4. Terraces features extracted from LiDAR-derived DTMs using landform curvature outlier's identification at large scale (see [Section 3.1](#)) for the Belgian (a) Soave-Fornace Michelin (b) and San Fruttuoso Abbey (c) study areas.

Table 3

Summary of the statistical assessment described in [Section 3.2](#), to verify the accuracy of the extracted features through the curvature method. * According to [Heipke et al. \(1997\)](#), the quality index is dimensionless and ranges between 0 (for no overlap between extracted and observed features) and 1 (for optimal overlap between extracted and observed feature; [Tarolli et al., 2012](#)). ** According to [Cohen \(1960\)](#), $k(x)$ (dimensionless) is the kappa standard and measures the accuracy with which the proposed approach can predict the extension of the area occupied by terrace riser edges or bases. The Cohen's kappa standard accuracy has values < 0 as indicating no agreement, to 1 as almost perfect agreement.

	Maximum curvature		Minimum curvature	
	Quality Index*	$k(X)$ **	Quality Index*	$k(X)$ **
Belgium	0.48	0.61	0.56	0.71
Soave-Fornace Michelin	0.66	0.77	0.70	0.80
San Fruttuoso Abbey	0.52	0.65	0.71	0.82

[et al., 2008](#)) outcropped sharply at the start of the steepest section of the valley side and was identified in six consecutive sample points between T3 to C7. In the upper section of the mid-slope (T3 and T4), the chalk created a relatively level sub-surface terrace which was comparable with the TS in zone T3 (closer to the terrace base), while at T4, the TS is deeper than the bedrock surface identified ([Table 4](#)). In the lower section of the mid-slope (T5), chalk was identified at approximately the same level of the TS, and unlike the upper section, did not remain semi-horizontal but dropped away in cores C5-7, meeting perfectly only in the intermediate part (i.e., zone C7 between the two terraces) of the TS. A sharply inclining sub-surface topography is indicated by a soil/sediment depth of more than 2.5 m in T6 and the evidence from C5-6, and is

well reflected in the TS reconstruction (i.e., shallow terrace deposits). In the lower valley and valley-bottom, coring and test-pitting demonstrated a reduced gradient but evidence of substantial downslope sediment transfer and a highly variable sub-surface topography, not easily shaped by TS. Indeed, between the foot of the lower terrace and extending outwards, approximately 40 m (C3 and C1) chalk was encountered at 0.30 m below ground level, demonstrating a moderately gentle sub-surface topography, which nicely coincides with the TS. However, in C8, chalk was found at 0.85 m, and in C2 at 1.20 m, suggesting an increase in sub-surface gradient, which dropped further towards the valley bottom as chalk was not identified in either C4 or T7 despite sediment recording to 2.60 m ([Table 4](#)). The extensive depth of colluvial and alluvial deposits in the lower valley and valley bottom area meant that we did not reach the underlying lithology. Therefore, it was difficult to reconstruct the TS, which should be much deeper. Without this data, we assigned the same starting depth as that identified in the T7 trench. Despite this difficulty across much of the Belgian site, the TS allowed the reconstruction of the original slope topography with sufficient accuracy and depicted areas of terrace remodelling through anthropogenic soil deposition (e.g., T6). It also identified reworking close to terrace bases (e.g., T3, C1, and C3), where bedrock outcrops closer to the surface and lateral sediment transfer across terraces and downslope through prolonged cultivation may have occurred modifying the existing ground surface.

At Soave-Fornace Michelin, the bedrock elevations within each of the sample trenches ([Fig. 5b](#); [Table 4](#)) demonstrate basal values which, mirror those determined from the TS, confirming the reliability of the methodology. The presence of more regularly shaped dry-stone terraces improved the identification of bases and, therefore, a more accurate reconstruction of the original sub-surface slope.

In the San Fruttuoso Abbey case study, no trenches or cores were

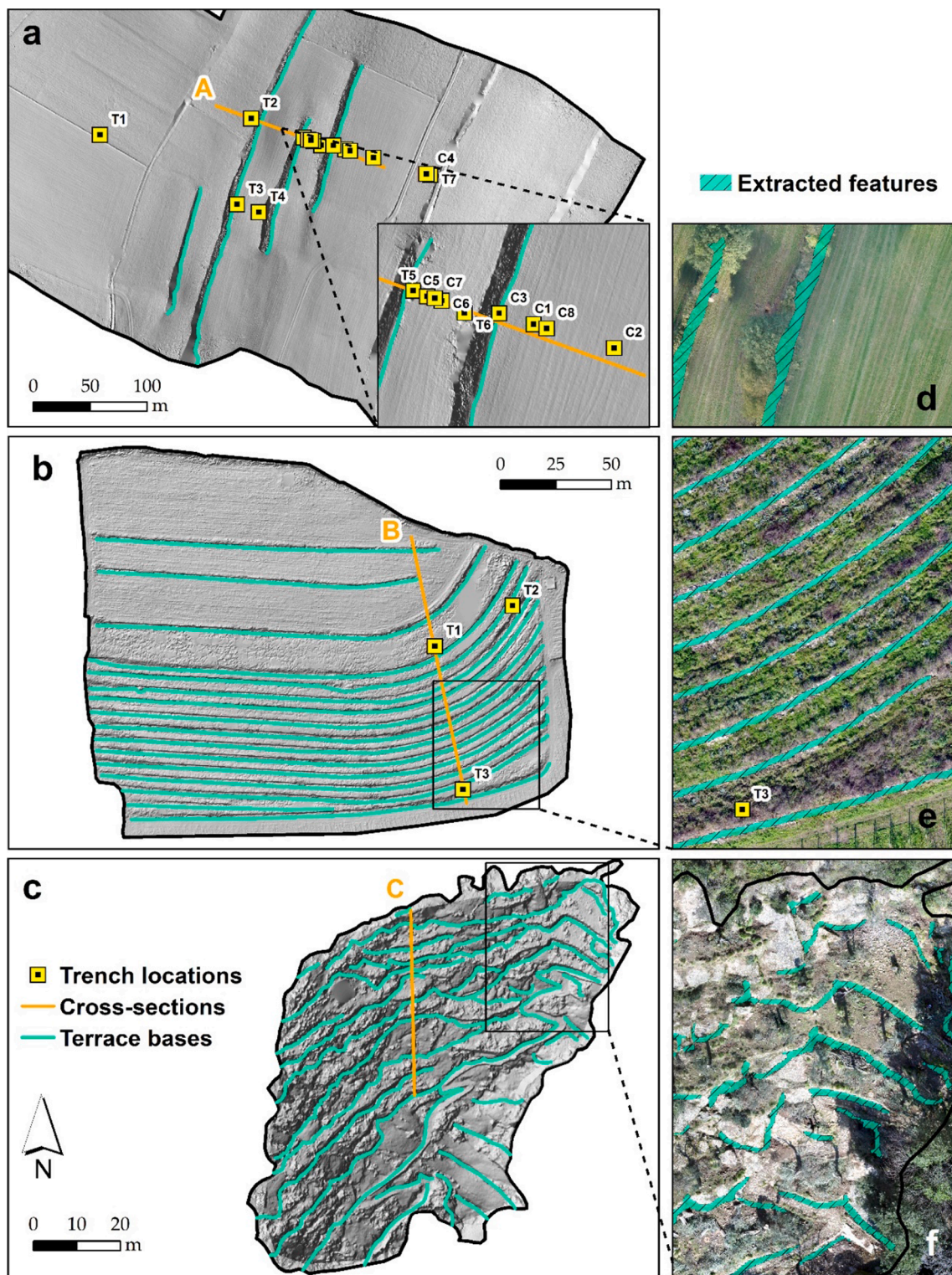


Fig. 5. 3D contour lines (a, b, and c) of the terrace and lynchet riser bases extracted from SfM-TLS surveys using minimum curvature values (d, e, and f) of very high-resolution DTMs (see Section 3.3) to reconstruct the theoretical surfaces for the Belgian (a and d) Soave-Fornace Michelon (b and e) and San Fruttuoso Abbey (c and f) terrace systems. For each study area a cross-section of terrace system was extracted to compare the real and the interpolated surface in Fig. 6.

dug, as it is clear that the terraces were built directly on bedrock. Looking at the different case studies, it is clear that the depths measured in the field support in broad terms the pattern of the hypothetical original slope reconstructed from terrace riser bases, and cases of deviation can be considered insignificant for estimating rapidly and raw volumes of the entire terraced system. The methodology used has

yielded satisfactory results that facilitate a rough estimate of the volumes of terraces at the landscape scale. It should be reiterated that this method was designed as an expeditious process exploiting geomorphometric data from simple DTMs. Uncertainties will increase where bedrock or terraces morphology are irregular and spatially heterogeneous (see the case of Belgium and San Fruttuoso). However, this

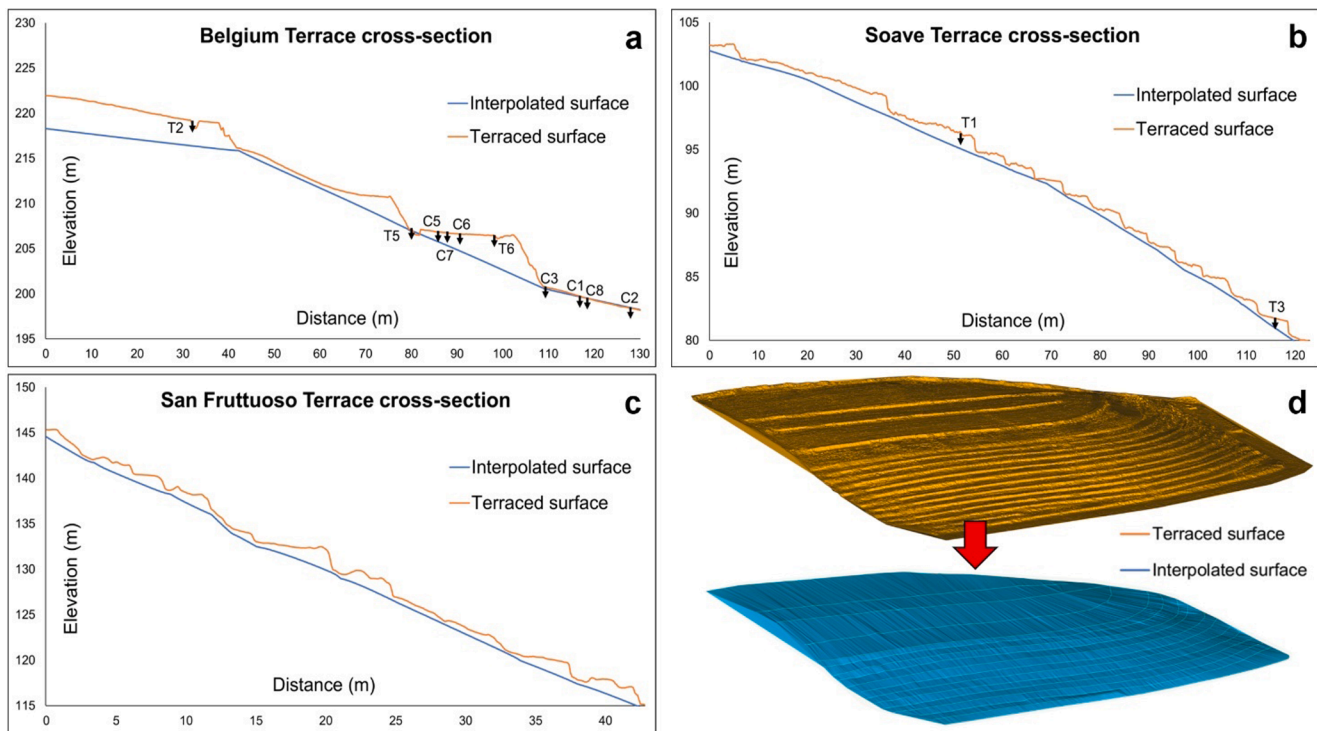


Fig. 6. Terrace and lynchet cross-section profile models of surface topography (blue) and interpolated sub-surface morphology (orange) alongside the positions of ground-truthing trenches and core sample points (Table 4) dug into the study areas (Fig. 2a, b, c, f and g) for the Belgian (a); Soave-Fornace Michelin (b) and San Fruttuoso Abbey (c) case study sites. (d) An example of 3D surface reconstruction of Soave-Fornace Michelin terraces and the theoretical surfaces obtained from the 3D contour lines of the terrace bases (see Section 3.3). (For interpretation of the references to colour in this figure legend, the reader is referred to the web version of this article.)

work and general observations (Brown et al., 2021) suggest that most terraces are built onto bedrock or stable weathered C horizon material where possible to prevent slipping. Indeed, in the case studies analysed (e.g., in Soave; see next Section 4.4), there were not the development of failure planes under the walls, but the wall collapses which indicated that the wall is stable, however the horizontal load is too great. Therefore, this could be a general situation and assumption for the terrace volume estimations which could be demonstrated in such cases by more detailed subsurface information through drilling, excavation or geophysical surveys. Certainly, there are different types of geophysical measurements, such as those used by Preti et al. (2018b), which can provide more complete data about the subsoil structure of terrace systems in order to better validate the volumetric results obtained, avoiding under- or over-estimates of soil. However, the use of more detailed geophysical analysis (e.g., seismic refraction measurements, electrical resistivity tomography or ground penetrating radar) would certainly increase costs and time in terms of the instrumentation required, and data processing. The rapid estimate of terrace volumes without subsurface data can still be beneficial as a rough reference for evaluating original pre-terrace slopes at the landscape scale.

4.3. DoD and volume computations

The utilisation of high-resolution surface DTMs and TS sub-surface models has enabled the creation of DoDs, allowing volume estimations of anthropogenic remodelling in terrace systems to be calculated with a decent degree of accuracy (Fig. 8; Table 5).

Volume statistics were estimated as differences between positive elevation values and negative ones. The former corresponding to the sediment accretion occurred on top of the hypothetical original slope, and the latter to the soil denudation and erosion resulted from the removal of material. The net volume difference represents the whole soil volume of a terrace or lynchet system. By multiplying it with the bulk

density, the total mass of mobilizable sediment is obtained (Table 5). The erosion volumes are very low compared to deposition values because the TSs are almost always lower than the real terraced layers, so the total net difference is positive. This means that the slopes were extensively remodelled, and there are large quantities of available soil. In contrast, when the real extant terrace surface is very similar to the modelled TS sub-strata or even has lower elevations, as demonstrated by the lower valley area in Belgium (Fig. 8a), there is evidence for extensive downslope sediment transfer through cultivation that might cover former lynchets or a terraced landscape. In other cases (e.g., Soave-Fornace Michelin and San Fruttuoso Abbey study areas; Fig. 8b and c), small, localised erosion zones can be observed, which may be due to soil removal to build terraces or possibly due to errors in the definition of the TS (e.g., errors in curvature extraction due to the presence of noise caused by vegetation and errors related to interpolation process or non-optimal point clouds filtering). It must be stressed that in the Portofino area soil may have been relocated from the valley or from the outside of the slope, as soil accumulation is hindered by the high slope gradient. Along the slopes close to the terraced area, Rellini et al. (2017) sampled soils at no more than 35 cm depth. Anyhow the origin of soil in terraces in such a steep slope is debated and the issue has not been solved yet. Besides, terraces are very old in this area and historical memory about terraces construction has been lost. The differences between volume estimation for thresholded and non-thresholded DoDs (i.e., Raw DoDs in Table 5) underline how the *minLoD* technique considers and reduces the uncertainties of DoDs. Several researchers stress the importance of thresholding (Anderson, 2019) and DTM uncertainty estimation, especially across steep slopes where the elevation error can be as much as twice that of low-angle-slopes, and horizontal error can have a greater impact on the observed elevation (Hodgson and Bresnahan, 2004; Cavalli et al., 2017). These problems were also highlighted by Heritage et al., (2009) and Milan et al., (2011), who showed that interpolation errors increase with local topographic variability. In Soave-Fornace

Table 4

Comparison between theoretical surfaces (see Section 3.3) and trenches/cores depths in the study areas. n/a means bedrock not encountered. “Trench/Core depth” refers to the overall depth of the excavation, while the “Trench/Core depth to bedrock” represents the depth at which the bedrock was found during the dig (in some cases the excavation continued even after the bedrock was found to analyse the subsoil structure). To assess the reliability of the methodology, the bedrock elevations within each of the sample trenches are compared to the TS values. The underlined values in table are used for the evaluation.

Study area	Field excavation			Theoretical surfaces			
	Trench/ Core No.	Field notes	Trench/Core depth (m)	Trench/Core depth to bedrock (m)	Elevation Trench/ Core bottom (m)	Elevation Trench/ Core bedrock (m)	Elevation interpolation surface (m)
Belgium	T1	Clay & gravel at 0.45 m, Lynchet	0.96	0.45	227.29	<u>227.80</u>	<u>227.80</u>
	T2	Gravel at 0.55 m, Lynchet	0.85	0.55	218.30	<u>218.60</u>	<u>216.53</u>
	T3	Chalk at 1.30 m, Terrace	1.50	1.30	215.48	<u>215.68</u>	<u>215.76</u>
	T4	Chalk at 1.30 m, Terrace	1.40	1.30	214.13	<u>214.23</u>	<u>210.94</u>
	T5	Chalk at 0.42 m, Terrace	0.57	0.42	206.60	<u>206.74</u>	<u>206.44</u>
	T6	2.50 m, no bedrock	2.50	n/a	204	<u>n/a</u>	<u>203.06</u>
	T7	2.60 m, no bedrock, valley bottom	2.60	n/a	190.30	<u>n/a</u>	<u>190.25</u>
	C1	Chalk at 0.30 m, lower valley	0.40	0.30	198.83	<u>198.93</u>	<u>199.26</u>
	C2	Chalk at 1.20 m, lower valley	1.40	1.20	195.01	<u>195.21</u>	<u>196.38</u>
	C3	Chalk at 0.30 m, lower valley	0.40	0.30	200.35	<u>200.45</u>	<u>200.23</u>
	C4	1.30 m, no bedrock valley bottom	1.30	n/a	191.93	<u>n/a</u>	<u>191.90</u>
	C5	Chalk at 0.60 m, Terrace	0.75	0.60	206.07	<u>206.22</u>	<u>205.85</u>
	C6	Chalk at 1.35 m, Terrace	1.50	1.35	205.10	<u>205.25</u>	<u>204.89</u>
	C7	Chalk at 1.10 m, Terrace	1.20	1.10	205.43	<u>205.53</u>	<u>205.34</u>
Soave-Fornace Michelin	T1	Rubby terra rossa 0.80 m to bedrock	0.80	0.80	95.44	<u>95.44</u>	<u>95.35</u>
	T2	Rubby terra rosa with collapse material: 1.40 m to bedrock	1.40	1.40	91.03	<u>91.03</u>	<u>91.34</u>
	T3	Rubby terra rossa 0.70 m to bedrock/rubble	0.70	0.70	80.91	<u>80.91</u>	<u>80.87</u>
San Fruttuoso Abbey	-	Terrace walls directly constructed on underlying lithology	-	-	-	-	-

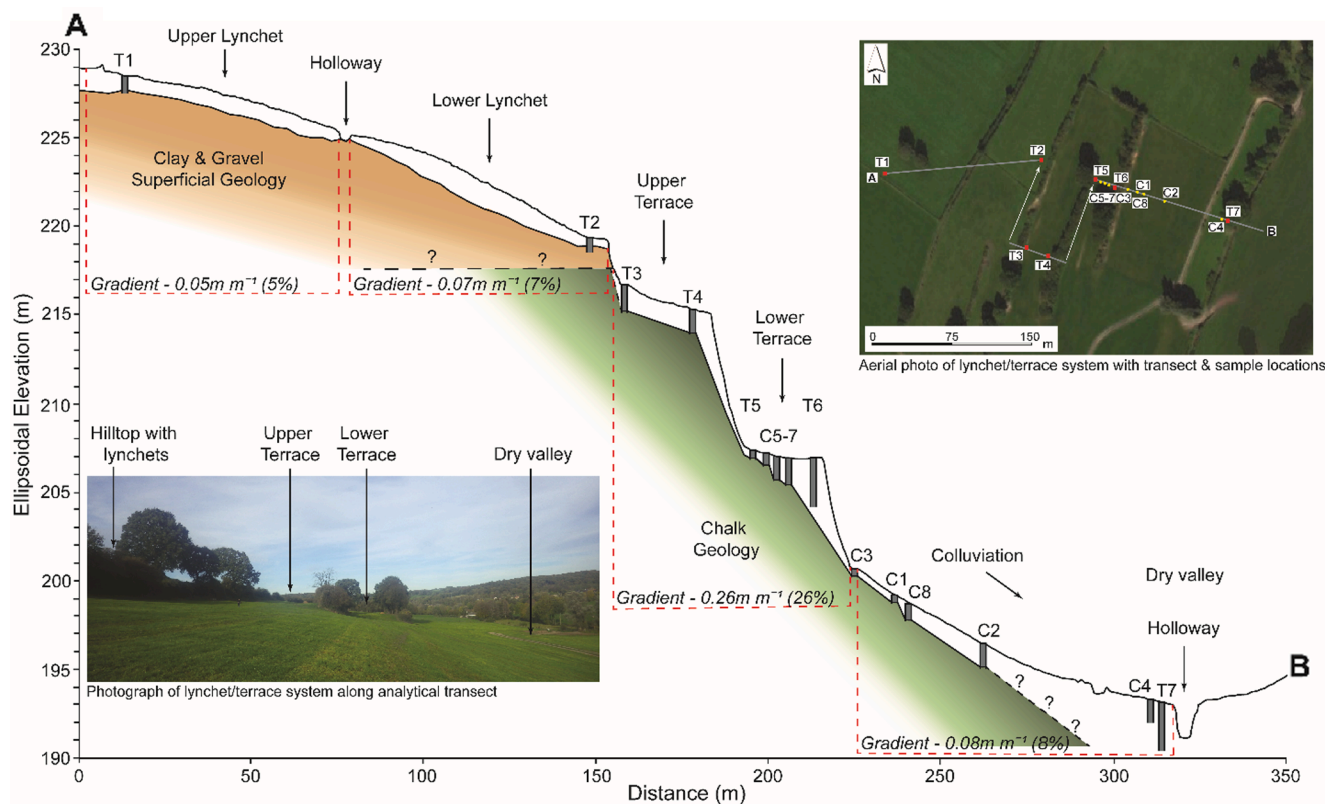


Fig. 7. Ground surface and sub-surface topography of the Sint-Marten Voerens lynchet/terrace system, Belgium along modelled transect with location of test pits (T1-7) and cores (C1-8).

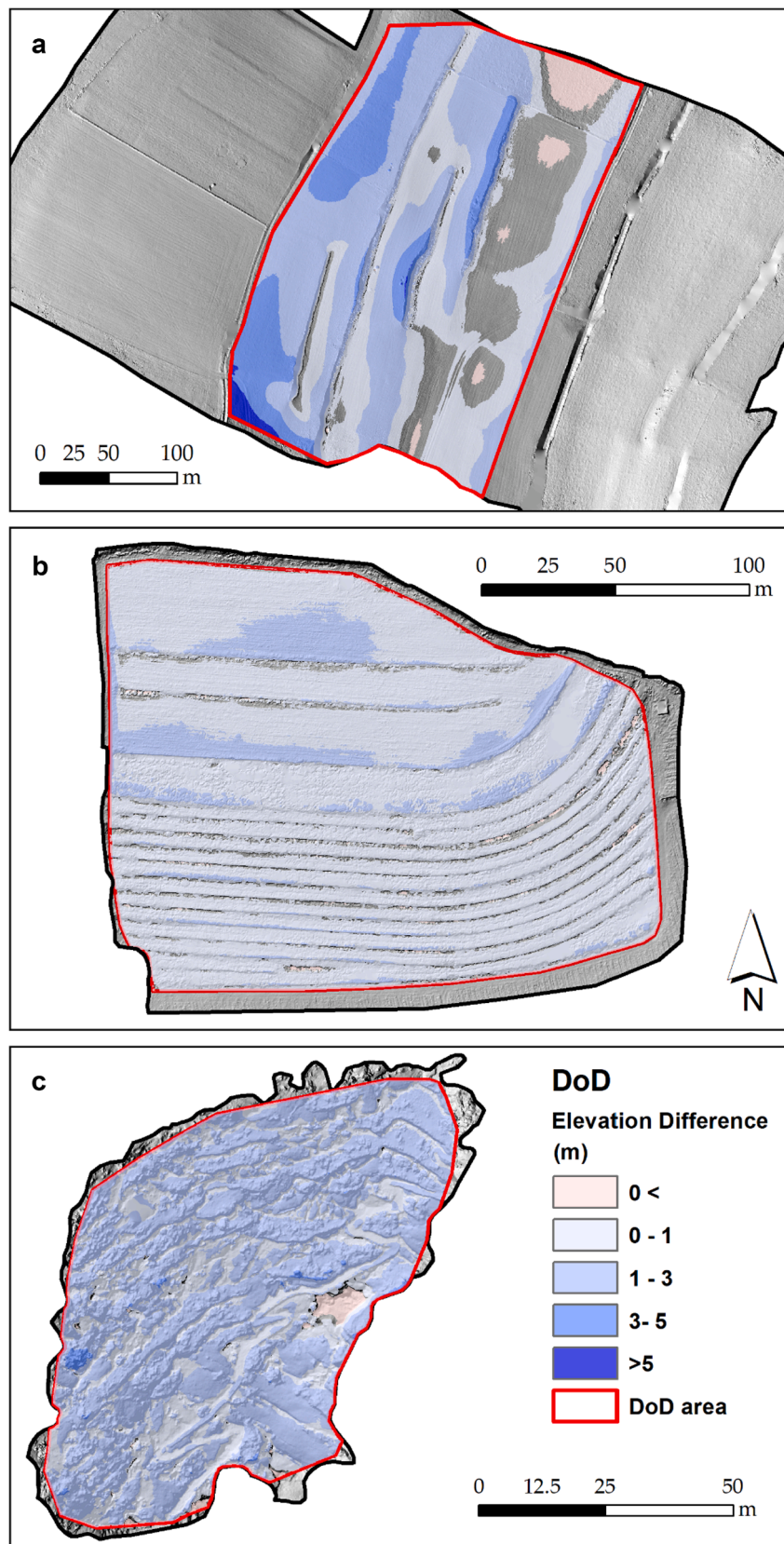


Fig. 8. Thresholded DoD ($t = 1.96$) for the Belgian (a) Soave-Fornace Michelin (b) and San Fruttuoso Abbey (c) terrace systems.

Table 5

Terrace and lynchet volume computation (erosion, deposition, and net volume changes) obtained from DoDs areas in Fig. 8. The \pm uncertainty of volumes was estimated considering a minLoD described in Section 3.4. *The bulk density data were obtained from soil samples of the trenches for Belgium and Soave-Fornace Michelon sites, while for San Fruttuoso Abbey study area the values came from literature (Relimi et al., 2017). The net volume differences represent the terrace and lynchet soil volume. ** SOC stocks were calculated by multiplying total soil mass (thresholded) with averaged SOC concentration (g/kg) of the terrace trenches. The original SOC profile data were presented in Table S1.

Study area	Volume				Thresholded DoD			Bulk density*		Mass		SOC stock	
	Raw DoD		Net Volume difference (m ³)		Erosion (m ³)	Deposition (m ³)	Net thickness equivalent (m)	kg/m ³	Raw	Thresholded	Tons	Mg	**
	Erosion (m ³)	Deposition (m ³)	Net Volume difference (m ³)	Net thickness equivalent (m)	Erosion (m ³)	Deposition (m ³)	Net Volume difference (m ³)						
Belgium	1392	90,827	89,434	1.38	1012 \pm 217	90117 \pm 5447	1.67 \pm 0.10	1380	123,418	122965 \pm 7522	1390 \pm 85		
Soave-Fornace Michelon	35	15,934	15,898	0.60	18 \pm 5	15827 \pm 1476	0.6 \pm 0.10	1020	16,215	16124 \pm 1506	282 \pm 26		
San Fruttuoso Abbey	27	6137	6109	1.29	26 \pm 3	6136 \pm 330	1.29 \pm 0.10	1250-1300	7636-7941	7636 \pm 413 7942 \pm 429	-		

Michelon and San Fruttuoso Abbey case studies, the uncertainties values of volume estimation are lower than in Belgium, where DTM errors were higher (see Table 2). Combined with the results obtained from the case study sites, this underlines the importance of the error analysis to derive better volume estimates of agricultural terrace and lynchet systems. Moreover, DoD investigations provide important information on the location of areas where soil storage is greater (e.g., within the hill-top lynchets in Belgium; Fig. 8a). This information is crucial for determining a range of parameters, such as sediment available for downslope movement to the calculation of loads and necessary strength of retaining walls or developing potential slip planes at the soil base. Additionally, it is the basis for the volumetric estimation of SOC storage in the terrace system. Here, SOC stocks were calculated by multiplying the total soil mass (thresholded) with averaged SOC concentration (g/kg) of the terrace trenches (Table 5). This estimation can only be viewed as a rough approximation as soil depth variability is not well represented. Still, even a rough calculation can provide useful preliminary information regarding quantification and mapping of the SOC stock in agricultural terrace systems especially for the effective estimation of SOC stock in terrace systems on a regional scale.

4.4. Connected sediment volumes

Regarding the mitigation of anthropogenic mismanagement (e.g., lack of terrace maintenance), terrace volumetric estimates, with information derived from geomorphometric indices, such as sediment connectivity, can make a significant contribution in the assessment of potential slope hazards. An example of this application is presented in Fig. 9, where IC was applied to the entire Soave-Fornace Michelon terrace system (Fig. 9b) as well as one specific area (Fig. 9c) of a dry-stone wall collapse (Fig. 9a). The wall failure was used as a target for IC computations to identify the upstream connected area as the source area for sediment eroded and transported through the collapsed terrace. Knowing the connected area, it is also possible to quantify the volume of sediments and associated SOC that could be mobilized and exported downstream after a terrace failure. DoD computation (Fig. 9d) for the area connected to the dry-stone wall collapse enables estimating volumes of sediment that can be mobilised in the short term (i.e., zones with very high values of IC; Table 6) and over more extended periods (i.e., zones with low IC values; Table 6). Fortunately, in this case, most of the sediments that can be mobilized after the wall failure have a medium-low connectivity due mainly to a not very high slope in this zone. Here, the dry-stone wall collapse (Fig. 9) can result in the mobilization of a total of 332 ± 24 m³ soil, corresponding to 5.91 ± 0.43 Mg C (Table 6). This information can help us understand the consequences of neglect or abandonment of terraces. As at the San Fruttuoso Abbey site, where gravity-induced processes and erosion dominate the geomorphic system, terrace collapse may cause localised small debris and soil accumulations but leave large bedrock surfaces exposed. The detail connected volumes would allow to plan preventive interventions or size works aimed at protecting the surrounding infrastructures both in the short and long term along San Fruttuoso steep slopes. Meanwhile, the mobilisation of these soil volumes and the SOC may increase soil nutrients and C losses, thereby threatening key ecosystem services provided by terraces such as erosion reduction and C storage (Wei et al., 2016; Stavi et al., 2019). The knowledge of the potential mobilised volumes after a terrace collapse could give realistic local information for system maintenance to stakeholders, and these computations can be used as reference and comparison values in soil erosion/C budget models for steep agricultural slopes. The data integration related to available terrace volumes, connectivity and C storage, could be the starting point for further studies. The literature lacks studies that integrate geomorphological and subsurface information that aim to understand and protect complex systems such as agricultural terraces.

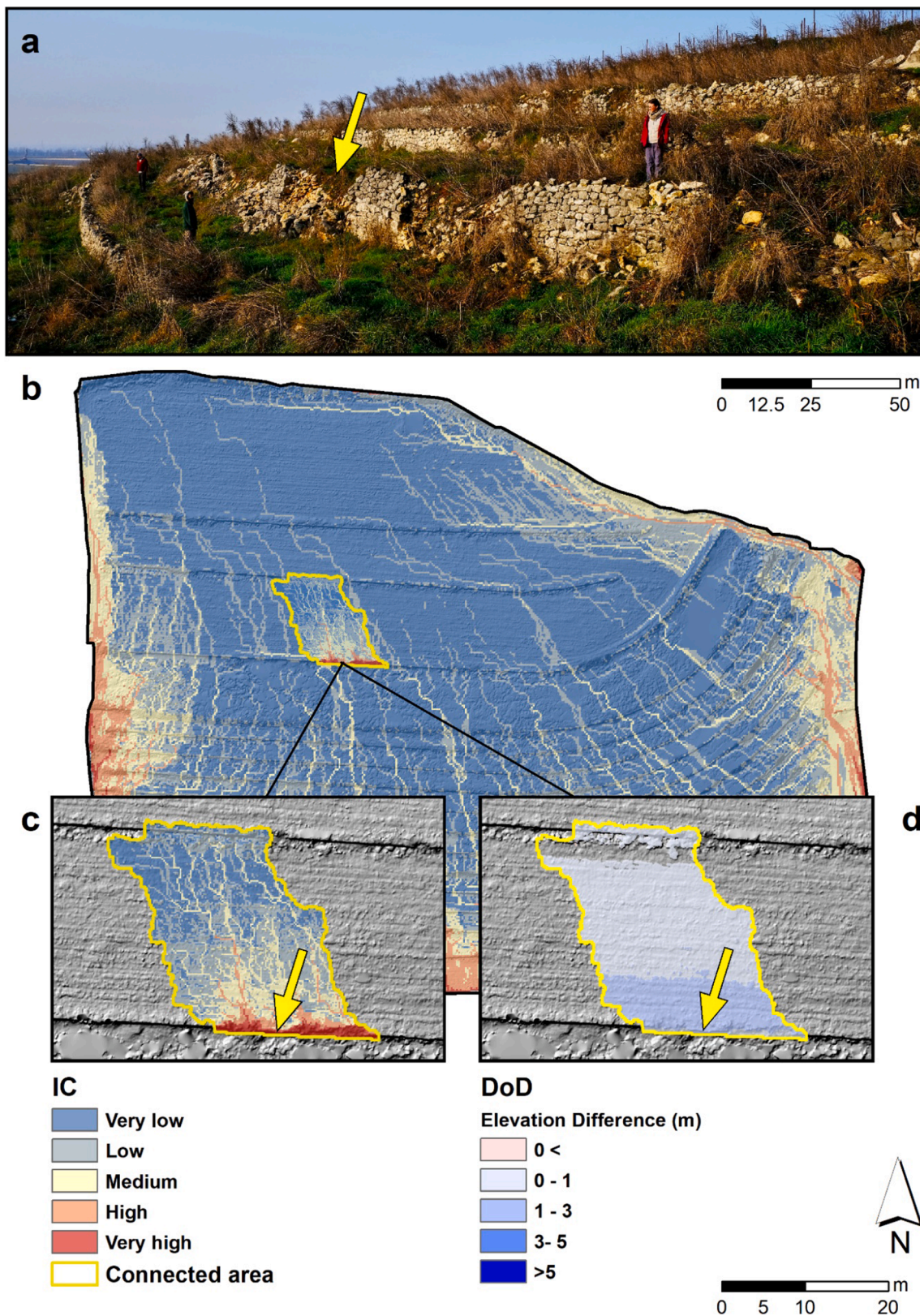


Fig. 9. Example of IC applied on the Soave-Fornace Michelon DTM (Fig. 5b), to identify and quantify the soil connected to a dry-stone wall collapse. The IC values have been classified into seven classes (very low, low, medium, medium, high and very high) based on the Natural Breaks classification methods. (a) Example of dry-stone wall collapse in Soave-Fornace Michelon; (b) IC map of Soave-Fornace Michelon terrace system where was identified the upstream area potentially connected in terms of sediment source with a dry-stone wall collapse; (c) Detail of IC map for which the volume of sediment (d) that can potentially be mobilised, has been calculated through DoD.

Table 6

Example of the potentially mobilizable volume based on the degree of IC of the area affected by a dry-stone wall collapse in Soave-Fornace Michelon. The \pm uncertainty of volumes were estimated considering a minLoD described in Section 3.4. The potential C mobilisation was calculated by multiplying total soil mass (thresholded) with averaged SOC concentrations (g/kg; see supplementary Table S1).

IC	Volume Thresholded DoD			Mass Thresholded	Potentially C mobilization
	Erosion (m ³)	Deposition (m ³)	Net Volume difference (m ³)	Tons	Mg
Very Low	0	58 \pm 7	58 \pm 7	59 \pm 7	1.03 \pm 0.12
Low	0	137 \pm 10	137 \pm 10	189 \pm 10	2.44 \pm 0.18
Medium	0	87 \pm 5	87 \pm 5	88 \pm 5	1.55 \pm 0.09
High	0	25 \pm 1	25 \pm 1	26 \pm 1	0.45 \pm 0.02
Very high	0	25 \pm 1	25 \pm 1	26 \pm 1	0.45 \pm 0.02
TOT	0	332 \pm 24	332 \pm 24	339 \pm 24	5.91 \pm 0.43

5. Conclusions

This research has combined extensive and detailed high-resolution topographic surveys with in-field sedimentological recordings to study the nature of sub-surface topographies of terraced agricultural landscapes. This work has enabled the mapping and characterisation of geomorphological features in a new wide-ranging perspective, as obtaining volume estimations are essential for the study of terrace origins and landscape evolution. The use of ALS data to derive geomorphometric parameters, such as curvature, enabled the identification of terraced systems even if they are abandoned or covered by uncontrolled vegetation at a large scale. The TLS and UAV-SfM surveys enabled the extraction of detailed, accurate high-resolution geomorphometric information from DTMs. By moving from terrace riser edges to terrace riser bases for the computation of minimum curvature, an innovative and rapid methodological workflow was developed to estimate the anthropogenic remoulded soil of terrace systems with appropriate accuracy, starting only from a simple DTM. Notably, the use of a coarse ground-truthing through field excavation and sampling has confirmed in broad terms the reliability of the methodology used across a range of sites with very specific terrace morphologies. In each case, it has confirmed the nature of the reconstructed, theoretical original slope. The developed workflow produced accurate DoDs, between the actual terrace DTMs and the theoretical DTMs generated from terrace riser bases, fundamental to estimate the soil volumes and mass used to remould the slopes at the landscape scale. Moreover, geomorphometric analysis through indices such as sediment connectivity also permitted the quantification of the volume of sediment transported downstream, with the associated and mobilized C, after a collapsed terrace. The volumetric data of agricultural terrace and lynchet systems, enriched by sediment connectivity analysis, represent the useful application and can now provide new benchmarks for soil erosion models and new perspectives for landowners and stakeholders for the management of these agricultural environments in terms of natural hazards (i.e., terraces as potential sediment source areas for hydro-erosive phenomena in the absence of terrace maintenance). Moreover, the quantification of terrace soil volumes provides valuable information to assess terrace ecosystem services such as the SOC sequestration and heritage services such as the history of human landscape impacts. Finally, the quantification of terrace soil volumes provides extremely useful standards for further multi-disciplinary analysis on the terrace sediments themselves, aiding physical geographers, geoarchaeologists, palaeo-environmentalists and landscape historians in the understanding of terrace systems and the impact of agricultural processes on the landscape.

Funding

This research was funded by the European Research Council, Advanced grant for the TerrACE research project (ERC-2017-ADG: 787790, 2019–2023; <https://www.terrace.no/>). This study was also partly supported by the project SOILUTION SYSTEM “Innovative solutions for soil erosion risk mitigation and a better management of

vineyards in hilly and mountain landscapes”, within Programma di Sviluppo Rurale per il Veneto 2014–2020 (www.soilutionsystem.com).

Declaration of Competing Interest

The authors declare that they have no known competing financial interests or personal relationships that could have appeared to influence the work reported in this paper.

Acknowledgement

The RECONNECT project (Regenerating ECOSystems with Nature-based solutions for hydro-meteorological risk rEDUCTION; European Union’s Horizon 2020 Research and Innovation Programme under grant agreement No 776866). The authors wish to thank Giacomo Crucil and He Zhang (Université Catholique de Louvain) for helping in the UAV Belgian surveys, and Eugenio Straffellini for his aid in the Italian field works. The authors also thank Consorzio Tutela Vini Soave e Recioto di Soave (<https://ilsoave.com>) for all the support provided during the field surveys carried out in the Soave Globally Important Agricultural Heritage Systems (GIAHS) site (Veneto region, Italy). We acknowledge the FAI (Fondo Ambiente Italiano) and the Agririfugio Molini for the availability and support given us to carry out the surveys in San Fruttuoso.

Appendix A. Supplementary material

Supplementary data to this article can be found online at <https://doi.org/10.1016/j.catena.2021.105687>.

References

- Anderson, S.W., 2019. Uncertainty in quantitative analyses of topographic change: error propagation and the role of thresholding. *Earth Surf. Process. Landforms* 44, 1015–1033. <https://doi.org/10.1002/esp.4551>.
- Arnáez, J., Lana-renault, N., Lasanta, T., Ruiz-flaño, P., Castroviejo, J., 2015. Catena Effects of farming terraces on hydrological and geomorphological processes. A review. *Catena* 128, 122–134. <https://doi.org/10.1016/j.catena.2015.01.021>.
- Borselli, L., Cassi, P., Torri, D., 2008. Prolegomena to sediment and flow connectivity in the landscape: a GIS and field numerical assessment. *Catena* 75, 268–277. <https://doi.org/10.1016/j.catena.2008.07.006>.
- Brasington, J., Langham, J., Rumsby, B., 2003. Methodological sensitivity of morphometric estimates of coarse fluvial sediment transport. *Geomorphology*. [https://doi.org/10.1016/S0169-555X\(02\)00320-3](https://doi.org/10.1016/S0169-555X(02)00320-3).
- Brasington, J., Vericat, D., Rychkov, I., 2012. Modeling river bed morphology, roughness, and surface sedimentology using high resolution terrestrial laser scanning. *Water Resour. Res.* <https://doi.org/10.1029/2012WR012223>.
- Brown, A.G., Fallu, D., Walsh, K., Cucchiaro, S., Tarolli, P., Zhao, P., Pears, B.R., van Oost, K., Snape, L., Lang, A., Albert, R.M., Alsos, I.G., Waddington, C., 2021. Ending the Cinderella status of terraces and lynchets in Europe: The geomorphology of agricultural terraces and implications for ecosystem services and climate adaptation. *Geomorphology* 379, 107579. <https://doi.org/10.1016/j.geomorph.2020.107579>.
- Cambi, M., Giambastiani, Y., Giannetti, F., Nuti, E., Dani, A., Preti, F., 2021. Integrated low-cost approach for measuring the state of conservation of agricultural terraces in tuscany, Italy. *Water (Switzerland)* 13, 1–18. <https://doi.org/10.3390/w13020113>.
- Camera, C., Djuma, H., Bruggeman, A., Zoumides, C., Eliades, M., Charalambous, K., 2018. Catena Quantifying the effectiveness of mountain terraces on soil erosion

- protection with sediment traps and dry-stone wall laser scans. *Catena* 171, 251–264. <https://doi.org/10.1016/j.catena.2018.07.017>.
- Carrivick, J.L., Smith, M.W., Quincey, D.J., 2016. Structure from Motion in the Geosciences. John Wiley & Sons, Ltd, Chichester, UK. <https://doi.org/10.1002/9781118895818>.
- Cavalli, M., Goldin, B., Comiti, F., Brardinoni, F., Marchi, L., 2017. Assessment of erosion and deposition in steep mountain basins by differencing sequential digital terrain models. *Geomorphology*. <https://doi.org/10.1016/j.geomorph.2016.04.009>.
- Cavalli, M., Trevisani, S., Comiti, F., Marchi, L., 2013. Geomorphometric assessment of spatial sediment connectivity in small Alpine catchments. *Geomorphology* 188, 31–41. <https://doi.org/10.1016/j.geomorph.2012.05.007>.
- Chen, D., Wei, W., Daryanto, S., Tarolli, P., 2020. Does terracing enhance soil organic carbon sequestration? A national-scale data analysis in China. *Sci. Total Environ.* 721, 137751 <https://doi.org/10.1016/j.scitotenv.2020.137751>.
- Cohen, J., 1960. A coefficient of agreement for nominal scales. *Educ. Psychol. Meas.* 20, 37–46. <https://doi.org/10.1177/001316446002000104>.
- Cucchiaro, S., Cavalli, M., Vericat, D., Crema, S., Llena, M., Beinat, A., Marchi, L., Cazorzi, F., 2018. Monitoring topographic changes through 4D-structure-from-motion photogrammetry: application to a debris-flow channel. *Environ. Earth Sci.* 77 <https://doi.org/10.1007/s12665-018-7817-4>.
- Cucchiaro, S., Fallu, D.J., Zhang, H., Walsh, K., Van Oost, K., Brown, A.G., Tarolli, P., 2020a. Multiplatform-SfM and TLS data fusion for monitoring agricultural terraces in complex topographic and landcover conditions. *Remote Sens.* 12, 1946. <https://doi.org/10.3390/rs12121946>.
- Cucchiaro, S., Fallu, D.J., Zhao, P., Waddington, C., Cockcroft, D., Tarolli, P., Brown, A.G., 2020b. SfM photogrammetry for GeoArchaeology, in: *Remote Sensing of Geomorphology*. Elsevier B.V., pp. 183–205. <https://doi.org/10.1016/B978-0-444-64177-9.00006-0>.
- De Blécourt, M., Hänsel, V.M., Brumme, R., Corre, M.D., Veldkamp, E., 2014. Soil redistribution by terracing alleviates soil organic carbon losses caused by forest conversion to rubber plantation. *For. Ecol. Manage.* 313, 26–33. <https://doi.org/10.1016/j.foreco.2013.10.043>.
- Diaz-Varela, R.A., Zarco-Tejada, P.J., Angileri, V., Loudjani, P., 2014. Automatic identification of agricultural terraces through object-oriented analysis of very high resolution DSMs and multispectral imagery obtained from an unmanned aerial vehicle. *J. Environ. Manage.* 134, 117–126. <https://doi.org/10.1016/j.jenvman.2014.01.006>.
- Evans, I.S., 1980. An integrated system of terrain analysis and slope mapping. *Zeitschrift für Geomorphol. Suppl. Stuttgart* 274–295.
- Faccini, F., Gabellieri, N., Paliaga, G., Piana, P., Angelini, S., Coratza, P., 2018. Geoheritage map of the portofino natural park (Italy). *J. Maps* 14, 87–96. <https://doi.org/10.1080/17445647.2018.1433561>.
- Godone, D., Giordan, D., Baldo, M., 2018. Rapid mapping application of vegetated terraces based on high resolution airborne lidar. *Geomatics. Nat. Hazards Risk* 9, 970–985. <https://doi.org/10.1080/19475705.2018.1478893>.
- Heipke, C., Mayer, H., Wiedemann, C., Jamet, O., 1997. Automated reconstruction of topographic objects from aerial images using vectorized map information. *Int Arch. Photogramm. Remote Sens. Spec. Inf. Sci* 23, 47–56.
- Heritage, G.L., Milan, D.J., Large, A.R.G., Fuller, I.C., 2009. Influence of survey strategy and interpolation model on DEM quality. *Geomorphology* 112, 334–344. <https://doi.org/10.1016/j.geomorph.2009.06.024>.
- Hodgson, M.E., Bresnahan, P., 2004. Accuracy of airborne Lidar-derived elevation: empirical assessment and error budget. *Photogramm. Eng. Remote Sens.* 70, 331–339. <https://doi.org/10.14358/PERS.70.3.331>.
- Höhle, J., Höhle, M., 2009. Accuracy assessment of digital elevation models by means of robust statistical methods. *ISPRS J. Photogramm. Remote Sens.* 64, 398–406. <https://doi.org/10.1016/j.isprsjprs.2009.02.003>.
- Javernick, L., Brasington, J., Caruso, B., 2014. Modeling the topography of shallow braided rivers using Structure-from-Motion photogrammetry. *Geomorphology* 213, 166–182. <https://doi.org/10.1016/j.geomorph.2014.01.006>.
- Lane, S.N., Westaway, R.M., Hicks, D.M., 2003. Estimation of erosion and deposition volumes in a large, gravel-bed, braided river using synoptic remote sensing. *Earth Surf. Process. Landforms* 28, 249–271. <https://doi.org/10.1002/esp.483>.
- Lin, H., 2011. Three principles of soil change and pedogenesis in time and space. *Soil Sci. Soc. Am. J.* 75, 2049–2070. <https://doi.org/10.2136/sssaj2011.0130>.
- Marteau, B., Vericat, D., Gibbins, C., Batalla, R.J., Green, D.R., 2017. Application of structure-from-Motion photogrammetry to river restoration. *Earth Surf. Process. Landforms* 42, 503–515. <https://doi.org/10.1002/esp.4086>.
- Milan, D.J., Heritage, G.L., Large, A.R.G., Fuller, I.C., 2011. Filtering spatial error from DEMs: Implications for morphological change estimation. *Geomorphology* 125, 160–171. <https://doi.org/10.1016/j.geomorph.2010.09.012>.
- Nyssen, J., Debever, M., Poesen, J., Deckers, J., 2014. Lynchets in eastern Belgium - a geomorphic feature resulting from non-mechanised crop farming. *Catena* 121, 164–175. <https://doi.org/10.1016/j.catena.2014.05.011>.
- Paliaga, G., Giostrella, P., Faccini, F., 2016. Terraced landscape as cultural and environmental heritage at risk: An example from Portofino Park (Italy). *Ann. ZA ISTRISKE MEDITERANSKE Stud. Hist. Sociol.* 26, 513–522.
- Paliaga, G., Luino, F., Turconi, L., De Graff, J.V., Faccini, F., 2020. Terraced landscapes on portofino promontory (Italy): identification, geo-hydrological hazard and management. *Water (Switzerland)* 12, 1–21. <https://doi.org/10.3390/w12020435>.
- Pijl, A., Quarella, E., Vogel, T.A., D'Agostino, V., Tarolli, P., 2021. Remote sensing vs. field-based monitoring of agricultural terrace degradation. *Int. Soil Water Conserv. Res.* 9, 1–10. <https://doi.org/10.1016/j.iswcr.2020.09.001>.
- Pirson, S., Spagna, P., Baelle, J.-M., Dambon, F., Gerrienne, P., Vanbrabant, Y., Yans, J., 2008. An overview of the geology of Belgium. *Mem. Geol. Surv. Belgium* 55, 26.
- Preti, F., Errico, A., Caruso, M., Dani, A., Guastini, E., 2018a. Dry-stone wall terrace monitoring and modelling. *L. Degrad. Dev.* 29, 1806–1818. <https://doi.org/10.1002/ldr.2926>.
- Preti, F., Guastini, E., Penna, D., Dani, A., Cassiani, G., Boaga, J., Deiana, R., Romano, N., Nasta, P., Palladino, M., Errico, A., Giambastiani, Y., Trucchi, P., Tarolli, P., 2018b. Conceptualization of water flow pathways in agricultural terraced landscapes. *L. Degrad. Dev.* 29, 651–662. <https://doi.org/10.1002/ldr.2764>.
- Rellini, I., Olivari, S., Scopesi, C., Firpo, M., 2017. The soils of the Portofino promontory (NW Italy): distribution, genesis and palaeoenvironmental implications. *Geogr. Fis. e Din. Quat.* 40, 211–232. <https://doi.org/10.4461/GFDQ2017.40.13>.
- Remondino, F., Nocerino, E., Toschi, I., Menna, F., 2017. A critical review of automated photogrammetric processing of large datasets. *ISPRS - Int Arch. Photogramm. Remote Sens. Spat. Inf. Sci. XLII-2/W5*, 591–599. <https://doi.org/10.5194/isprs-archives-XLII-2-W5-591-2017>.
- Rosenbaum, M., McMillan, A., Powell, J., Cooper, A., Culshaw, M., Northmore, K., 2003. Classification of artificial (man-made) ground. *Eng. Geol.* 69, 399–409. [https://doi.org/10.1016/S0013-7952\(02\)0282-X](https://doi.org/10.1016/S0013-7952(02)0282-X).
- Shi, P., Zhang, Y., Li, P., Li, Z., Yu, K., Ren, Z., Xu, G., Cheng, S., Wang, F., Ma, Y., 2019. Distribution of soil organic carbon impacted by land-use changes in a hilly watershed of the Loess Plateau. *China. Sci. Total Environ.* 652, 505–512. <https://doi.org/10.1016/j.scitotenv.2018.10.172>.
- Sofia, G., 2020. Combining geomorphometry, feature extraction techniques and Earth-surface processes research: the way forward. *Geomorphology* 355, 107055. <https://doi.org/10.1016/j.geomorph.2020.107055>.
- Sofia, G., Fontana, G.D., Tarolli, P., 2014a. High-resolution topography and anthropogenic feature extraction: testing geomorphometric parameters in floodplains. *Hydrol. Process.* 28, 2046–2061. <https://doi.org/10.1002/hyp.9727>.
- Sofia, G., Marinello, F., Tarolli, P., 2014b. A new landscape metric for the identification of terraced sites: The slope local length of auto-correlation (SLLAC). *ISPRS J. Photogramm. Remote Sens.* 96, 123–133. <https://doi.org/10.1016/j.isprsjprs.2014.06.018>.
- Stavi, I., Gusarov, Y., Halbac-Cotoara-Zamfir, R., 2019. Collapse and failure of ancient agricultural stone terraces: On-site geomorphic processes, pedogenic mechanisms, and soil quality. *Geoderma* 344, 144–152. <https://doi.org/10.1016/j.geoderma.2019.03.007>.
- Tarolli, P., Cao, W., Sofia, G., Evans, D., Ellis, E.C., 2019. From features to fingerprints: A general diagnostic framework for anthropogenic geomorphology. *Prog. Phys. Geogr. Earth Environ.* 43, 95–128. <https://doi.org/10.1177/0309133318825284>.
- Tarolli, P., Preti, F., Romano, N., 2014. Terraced landscapes: From an old best practice to a potential hazard for soil degradation due to land abandonment. *Anthropocene* 6, 10–25. <https://doi.org/10.1016/j.ancene.2014.03.002>.
- Tarolli, P., Sofia, G., Dalla Fontana, G., 2012. Geomorphic features extraction from high-resolution topography: Landslide crowns and bank erosion. *Nat. Hazards* 61, 65–83. <https://doi.org/10.1007/s11069-010-9695-2>.
- Tucci, G., Parisi, E.L., Castelli, G., Errico, A., Corongiu, M., Sona, G., Viviani, E., Bresci, E., Preti, F., 2019. Multi-sensor UAV application for thermal analysis on a dry-stone terraced vineyard in rural Tuscany landscape. *ISPRS Int. J. Geo-Information* 8. <https://doi.org/10.3390/ijgi8020087>.
- Tukey, J.W., n.d. Exploratory data analysis.
- Vericat, D., Smith, M.W., Brasington, J., 2014. Patterns of topographic change in sub-humid badlands determined by high resolution multi-temporal topographic surveys. *Catena* 120, 164–176. <https://doi.org/10.1016/j.catena.2014.04.012>.
- Vericat, D., Wheaton, J.M., Brasington, J., 2017. Revisiting the morphological approach. *Gravel-Bed Rivers*. <https://doi.org/10.1002/9781118971437.ch5>.
- Walter, C., Merot, P., Layer, B., Dutin, G., 2003. The effect of hedgerows on soil organic carbon storage in hillslopes. *Soil Use Manag.* 19, 201–207. <https://doi.org/10.1079/sum2002190>.
- Wei, W., Chen, D., Wang, L., Daryanto, S., Chen, L., Yu, Y., Lu, Y., Sun, G., Feng, T., 2016. Global synthesis of the classifications, distributions, benefits and issues of terracing. *Earth-Science Rev.* 159, 388–403. <https://doi.org/10.1016/j.earscirev.2016.06.010>.
- Wei, Z., Han, Y., Li, M., Yang, K., Yang, Y., Luo, Y., Ong, S.H., 2017. A small UAV Based multi-temporal image registration for dynamic agricultural terrace monitoring. *Remote Sens.* 9 <https://doi.org/10.3390/rs9090904>.
- Welemariam, M., Kebede, F., Bedadi, B., Bihane, E., 2018. Enclosures backed up with community-based soil and water conservation practices increased soil organic carbon stock and microbial biomass carbon distribution, in the northern highlands of Ethiopia. *Chem. Biol. Technol. Agric.* 5, 1–11. <https://doi.org/10.1186/s40538-018-0124-1>.
- Wheaton, J.M., Brasington, J., Darby, S.E., Sear, D.A., 2010. Accounting for uncertainty in DEMs from repeat topographic surveys: Improved sediment budgets. *Earth Surf. Process. Landforms* 35, 136–156. <https://doi.org/10.1002/esp.1886>.
- Wood, J., 1996. *The geomorphological characterisation of digital elevation models*. University of Leicester.
- Xu, G., Lu, K., Li, Z., Li, P., Wang, T., Yang, Y., 2015. Impact of soil and water conservation on soil organic carbon content in a catchment of the middle Han River. *China. Environ. Earth Sci.* 74, 6503–6510. <https://doi.org/10.1007/s12665-015-4749-0>.
- Zhao, P., Fallu, D.J., Cucchiaro, S., Tarolli, P., Waddington, C., Cockcroft, D., Snape, L., Lang, A., Doetterl, S., Brown, A.G., Van Oost, K., 2021. SOC stabilization mechanisms and temperature sensitivity in old terraced soils, *Biogeosciences Discuss.* [preprint], <https://doi.org/10.5194/bg-2021-205>, in review.